Interation Notes

Notes 451

August 1985

THE CURRENT INDUCED IN AN INFINITELY LONG AND FINITELY CONDUCTING WIRE OVER A PLANE AND HOMOGENEOUS EARTH DUE TO A UNIFORM PLANE WAVE HAVING VARIOUS WAVESHAPES (EMP)*

H. P. Neff, Jr.
University of Tennessee
Knoxville, Tennessee

D. A. Reed
University of Tennessee
Knoxville, Tennessee

Abstract

The time-domain current induced in an infinitely long and finitely conducting wire over a plane and homogeneous earth in the presence of a plane electromagnetic wave with its magnetic field parallel to the earth and perpendicular to the wire axis is determined for several electric field (time-domain) waveshapes. The time-domain current is found by numerical inversion of the Fourier transform. Results indicate that electric field waveshapes with large fall times induce the largest peak currents in the wire.

*Research sponsored by the Office of Energy Storage and Distribution, U.S. Department of Energy, under Contract No. DE-AC05-840R21400 with Martin Marietta Energy Systems, Inc.

I. INTRODUCTION

When an infinitely-long, finitely-conducting, and circular-cylindrical, wire over a plane homogeneous earth is exposed to a uniform plane wave in the form of a pulse, the current induced in the wire takes the form of a pulse. This current can be calculated exactly in phasor form under ideal conditions. The time-domain current is then calculated numerically by means of the inverse Fourier transform. This current waveshape depends on the assumed waveshape of the electric field of the plane wave. It is the purpose of this study to determine which characteristics of the waveshape of the electric field are most important in determining the peak value of the induced wire current.

II. DESCRIPTION OF THE TIME-DOMAIN ELECTRIC FIELD

The infinitely long wire lies parallel to the plane earth at a height h. It has a radius a and conductivity σ_w. The earth has conductivity σ ($\mho$ /m) relative permittivity ε_R, and permeability $\mu_o = 4\pi \times 10^{-7}$ (H/m) (all assumed to be constant). The incident electromagnetic field is assumed to be that of a uniform plane wave with vertical polarization. That is, the electric field vector lies in the plane that is perpendicular to the earth and contains the wire axis. The Poynting vector is inclined at an angle θ with respect to the wire axis, while the magnetic field vector is parallel to the ground plane. This is shown in Figure 1.

Several different time-domain waveforms for the electric field were used in this study. The first (A) is encountered frequently in EMP studies, and so most of the discussion to follow will compare the other waveforms to this one.

$$\text{A} \qquad e_o(t) = 52.5\ (e^{-4 \times 10^6 t} - e^{-478 \times 10^6 t})u(t) \qquad \text{(kV/m)}$$

This is a standard double exponential waveform that attains a peak value of approximately 50 (kV/m) in approximately 10 (ns), and then decays to 25 (kV/m) after a total time of about 186 (ns). The 10%-90% rise time is 4.13 (ns). It is shown in Figure 2.

$$\text{B} \qquad e_o(t) = 64.25\ (e^{-30 \times 10^6 t} - e^{-476 \times 10^6 t})u(t)$$

The peak value is 50 (kV/m) at 6.2 (ns), while the fall time to 50% of the peak value is 31 (ns), and the 10%-90% rise time is 3.15 (ns). This is shown in Figure 3.

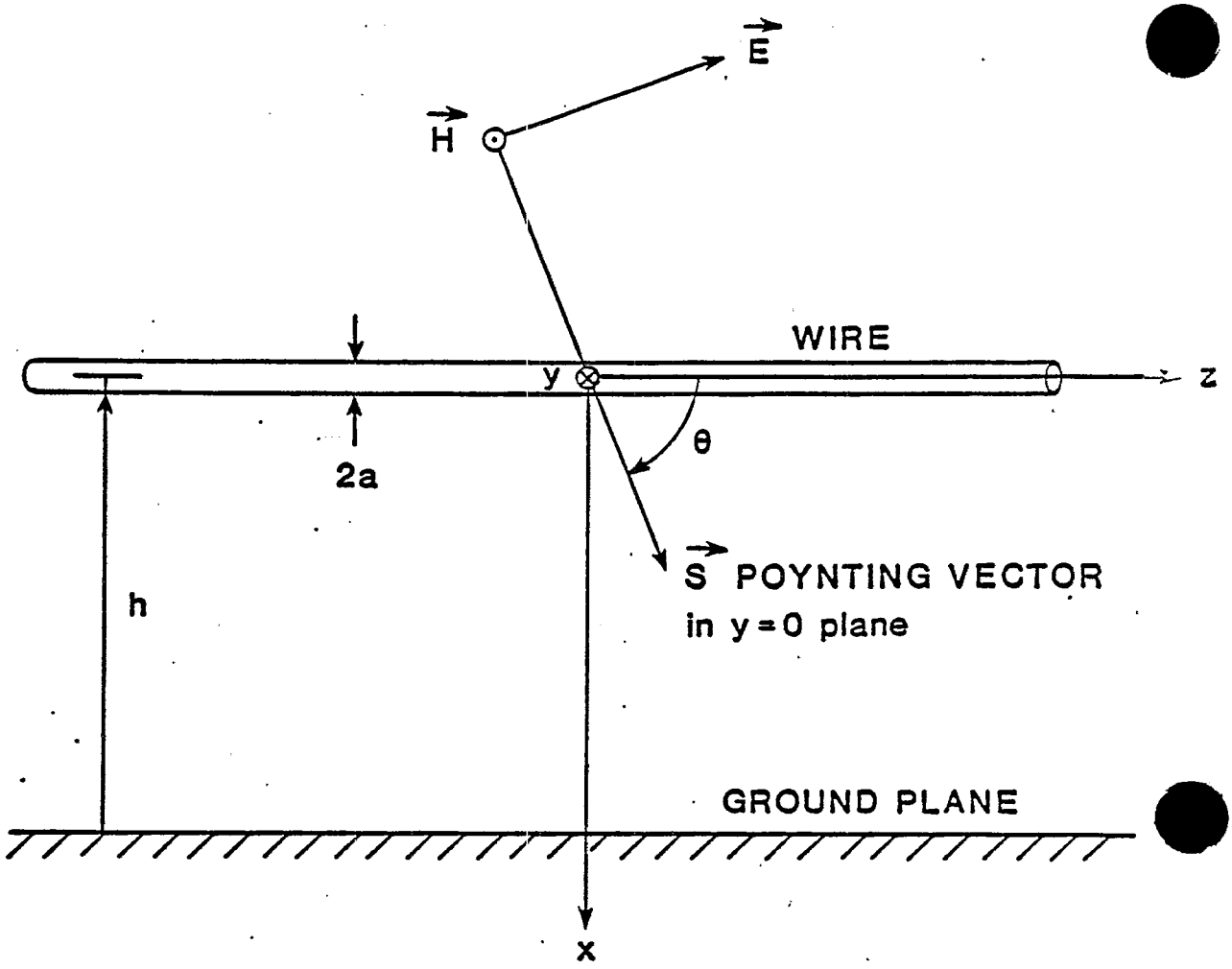

Figure 1. Geometry of the Problem.

C $$e_0(t) = 25.73\,[1-\cos(\pi t/5\times10^{+9})][u(t)-u(t-5.02\times10^{-9})]$$

$$+\,52.5\,e^{-4\times10^{6}t}\,u(t-5.02\times10^{-6}) \quad \text{(kV/m)}$$

This waveshape is formed by connecting two analytic forms at t = 5.02 (ns) so that they, along with their first derivatives, are equal there. The first analytic form is zero at t=0, and, in particular, its first derivative is zero at t=0. The decay is almost identical to that for A. The peak value occurs at exactly 5 (ns). The 10%-90% rise time is 2.95 (ns). It is shown in Figure 4. Notice that it is virtually indistinguishable (for the time scale used) from the electric field in A.

D $$e_0(t) = 26.25\,[1-\cos(\pi t/5\times10^{+9})][u(t)-u(t-5\times10^{-9})]$$

$$+\,52.5\,e^{-4\times10^{6}t}\,u(t-5\times10^{-9}) \quad \text{(kV/m)}$$

This waveform is essentially the same as that for C, except that the first derivatives of the two analytic forms are not equal at their junction [t = 5 (ns)]. It is shown in Figure 5.

E $$e_0(t) = 52.5\,(e^{-4\times10^{6}t}-e^{-478\times10^{6}t})[u(t)-u(t-1.393\times10^{-6})]$$

$$+\,200\,[u(t-1.393\times10^{-6})-u(t-0.1)] \quad \text{(kV/m)}$$

This waveform is identical to that for A, except that when it falls to 200 (V/m), it remains constant at 200 (V/m) until 0.1 (s), whereupon it stops. It is shown in Figure 6. Notice that the long "tail" of this waveform does not show in Figure 6 since it does not begin until t = 1.393 μs.

F $$e_0(t) = 100\sin(\pi\times10^{8}t)\cos(6\pi\times10^{10}t)\,[u(t)-u(t-10^{-8})] \quad \text{(kV/m)}$$

This is 30 (GHz) microwave signal whose amplitude is varied according to $\sin(\pi \times 10^8 t)$. It is gated on at t=0 and off at t = 10 (ns). Figure 7 shows the normalized waveforms A through E plotted together for purposes of comparison. Notice the scale change at t = 20 ns!

The important time-domain features of these waveforms are listed in Table 1. The frequency response characteristics (Fourier transform) are shown in Appendix A, Figures A.1 through A.5 (magnitude in decibels versus angular frequency on a logarithmic scale).

Table 1. Time-Domain Features of the Electric Field

Waveform	10%-90% rise time, T_r ns	Time to peak, T_p ns	Time to $\frac{1}{2} E_{peak}$ Fall time ns
A	4.128	10.09	185.5
B	3.151	6.198	31.47
C	2.952	5.00	178.3
D	2.952	5.00	173.3
E	4.128	10.09	185.5

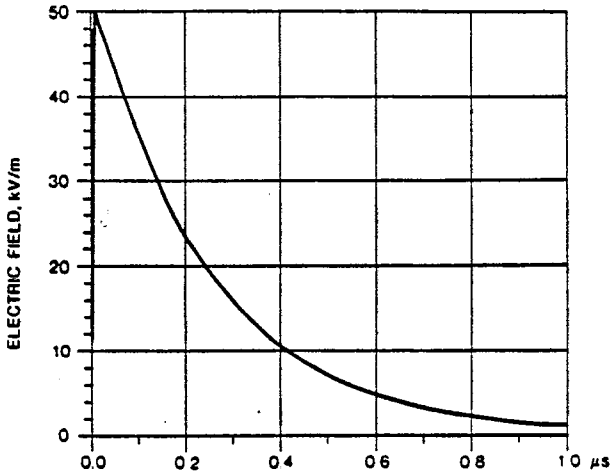

Figure 2. Electric field, case A.

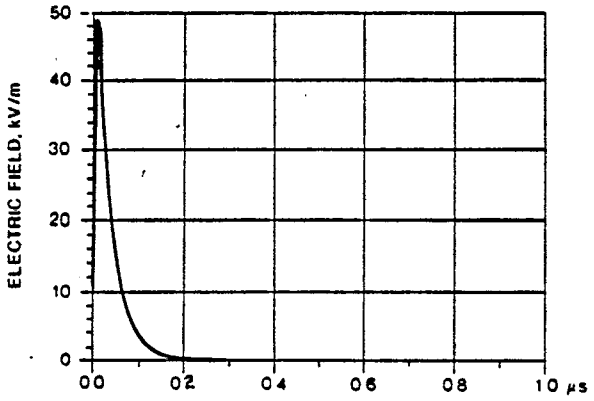

Figure 3. Electric field, case B.

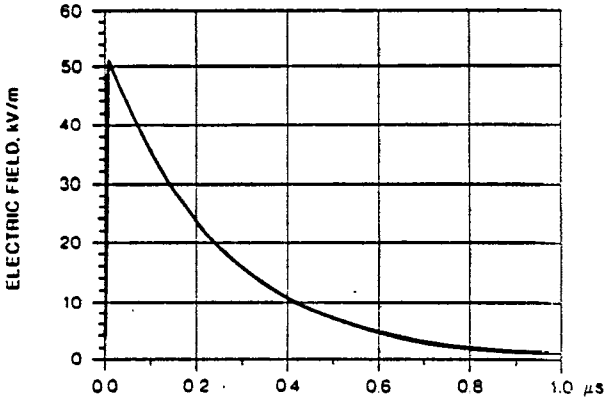

Figure 4. Electric field, case C.

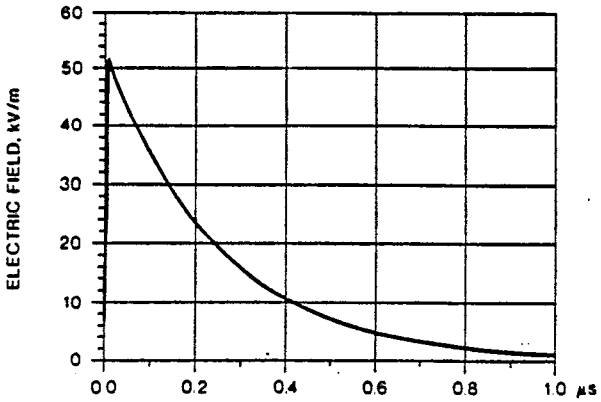

Figure 5. Electric field, case D.

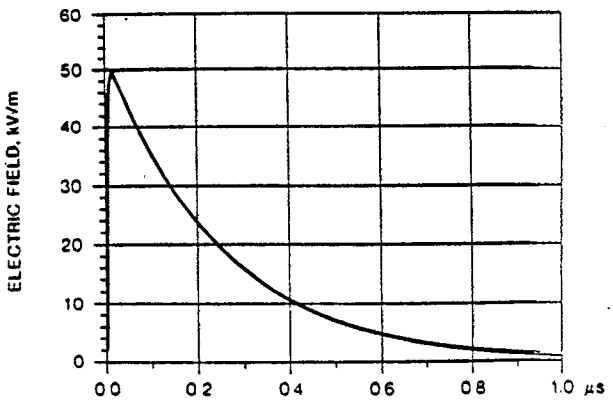

Figure 6. Electric field, case E.

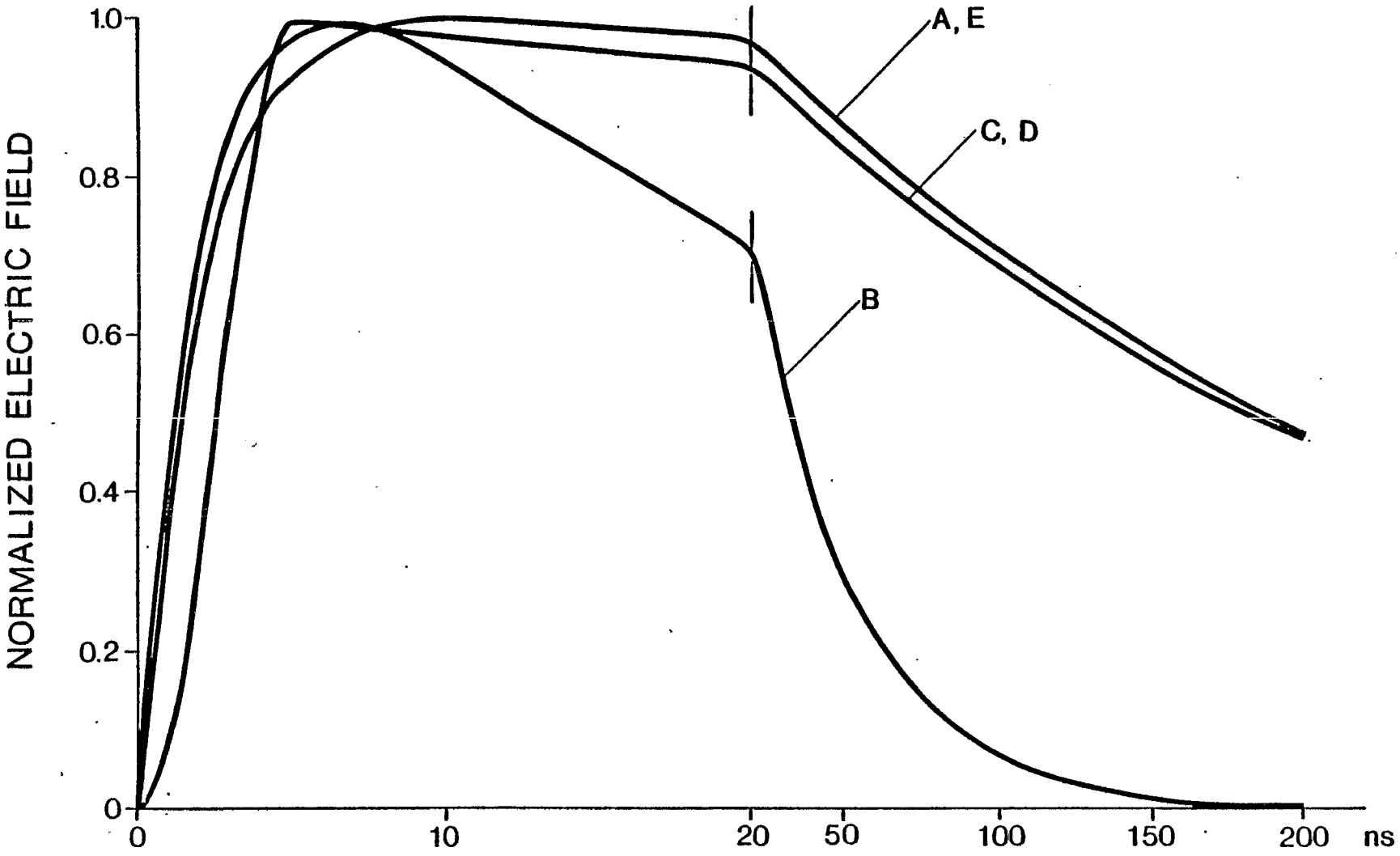

Figure 7 A comparison of the Electric Fields.

III. CALCULATION OF THE CURRENT

The current induced in an infinitely long and isolated circular conductor of radius a and conductivity σ_w from the plane wave described in the preceding section is given exactly by[1]

$$I_1(z,\omega) = \frac{4E_o(\omega)}{\omega \mu_o \sin\theta} e^{-jk_z z} \frac{1}{H_o^{(2)}(k_\rho a) - \frac{k'_\rho \varepsilon_o}{k_\rho \varepsilon'} \frac{J_o(k'_\rho a)}{J_1(k'_\rho a)} H_1^{(2)}(k_\rho a)} \tag{1}$$

in phasor form. It is also shown in reference 1 that, for any reasonable conductor size and conductivity, (1) reduces to a simpler approximate form:

$$I_1(z,\omega) = \frac{4E_o(\omega)}{\omega \mu_o \sin\theta} e^{-jk_z z} \frac{1}{H_o^{(2)}(k_\rho a) - j \frac{1}{60\pi \sigma_w a \sin\theta} H_1^{(2)}(k_\rho a)} \tag{2}$$

In these equations

$$\mu_o = 4\pi \times 10^{-7} \text{ (H/m)}$$

$$\varepsilon_o \approx 10^{-9}/36\pi \text{ (F/m)}$$

$$k = \omega\sqrt{\mu_o \varepsilon_o} \quad (m^{-1})$$

$$k_z = k\cos\theta \quad (m^{-1})$$

$$k_\rho = k\sin\theta \quad (m^{-1})$$

$$k'_\rho = k\sqrt{\varepsilon'/\varepsilon_o - \cos^2\theta} \quad (m^{-1})$$

$$\varepsilon' = \varepsilon_o(1 + \sigma_w/j\omega\varepsilon_o) \text{ (F/m)}$$

J_0, J_1, $H_o^{(2)}$, and $H_1^{(2)}$ are Bessel and Hankel functions, respectively.

It is expeditious to make two basic assumptions when considering the effect of the ground and the reflected wave[2]. First, it assumed that the ground "constants" are truly constant, being independent of position, direction, frequency, and the strength of the applied field. In the absence of detailed knowledge of the ground this is a reasonable assumption. Second, the field that is scattered from the wire, reflected from the ground, and incident again on the wire, is ignored. This appears to be a reasonable assumption because of the spreading effect of cylindrical waves, but its effects will be investigated in a future report. With these assumptions, the current induced in the wire from the ground reflected plane wave is given by

$$I_2(z,\omega) = I_1(z,\omega)\,\Gamma_H(\omega)\,e^{-j2\omega\sqrt{\mu_o\varepsilon_o}\;h\sin\theta} \tag{3}$$

where the reflection coefficient (for H parallel to the ground) is given by[3,4]

$$\Gamma_H(\omega) = -\frac{n^2\sin\theta - \sqrt{n^2 - \cos^2\theta}}{n^2\sin\theta + \sqrt{n^2 - \cos^2\theta}} \tag{4}$$

where

$$n^2 = \varepsilon_{Re} - j\,\sigma_e/(\omega\varepsilon_o)$$

$\sigma_e = \sigma$ = earth conductivity (υ/m)

$\varepsilon_{Re} = \varepsilon_R$ = relative earth permittivity

$\varepsilon_o = 10^{-9}/(36\pi)$ (F/m)

The total current in the wire is

$$I(z,\omega) = I_1(z,\omega) + I_2(z,\omega) \tag{5}$$

The time-domain current in the wire is given by

$$i(z,t) = F^{-1}\{I_1(z,\omega)\} + F^{-1}\{I_2(z,\omega)\}$$

$$= F^{-1}\{I_1(z,\omega)\} + F^{-1}\{I_1(z,\omega)\,\Gamma_H(\omega)\}_{t \to t - 2h\sqrt{\mu_o \varepsilon_o}\sin\theta} \qquad (6)$$

The inversion integral is

$$i(z,t) = \frac{1}{\pi}\int_0^\infty |I(z,\omega)|\cos(t\omega + \underline{|I(z,\omega)}))d\omega \qquad (7)$$

and was evaluated numerically.

IV. RESULTS

The parameters that were chosen for this study are the angle θ that the wave vector makes with the wire, the ground conductivity σ, and the relative permittitivity of the ground ε_R. The height (h) of the wire above the ground (Figure 1) was chosen to be 10 meters, the radius of the wire (a) was chosen to be 0.715 centimeters, and the conductivity of the wire was chosen to be 2.31×10^7 mhos/meter. The wire radius and conductivity, within reasonable limits, have only a minor effect on the induced current, whereas, the time delay of the ground-reflected wave is directly proportional to the wire height, as equation (3) shows.

The Brewster angle (or polarizing angle) is the angle for which there is no reflected wave when the reflecting medium is lossless and when the magnetic field vector is parallel to the ground. It is given by

$$\theta_B = \cos^{-1}\sqrt{\frac{\varepsilon_R}{\varepsilon_R + 1}}$$

Since the parameter ε_R was chosen to be 10 and 15 in this work, the Brewster angles are 17.55°, and 14.48°, respectively. The ground conductivity was chosen to be 10^{-3} and 10^{-2} mhos per meter, and because the ground is not lossless, there is no true Brewster angle, although the reflected wave behaves differently at high frequencies for this angle. The magnitude (in decibels) and angle (in degrees) of $\Gamma_H(\omega)$ are plotted against angular frequency on a logarithmic scale in Figures A.6 through A.13 (Appendix A). The parameter θ was given the values 10°, 14.48°, 17.55°, 20°, 36° and 90°. The large step

between 36° and 90° is used since the induced current does not change much with θ when θ is near 90°.

Figures 8 through 31 show the induced wire current for waveshapes A, B, and C. Notice, first of all, that the currents for A and C are indistinguishable for all practical purposes, and this indicates that it makes little difference how the electric field reaches its peak value, since waveforms A and C both begin at zero (at $t = 0$) and ultimately reach the same peak value, but are entirely different for times up to the peak. On the other hand, these waveforms are identical, so far as the decay is concerned. Thus, it would appear that the decay (or fall time) is the important factor in determining peak induced current. This fact is emphasized when the current for A (or C) is compared to that for B. The peak current for A is from 1.5 to 4 times larger than that for B though they have almost the same peak field, and this is because the fall time for waveshape A is about 6 times as large. Since waveshapes C and D are almost identical, the currents for D will be almost the same as those for A and C. Calculations have verified this, and the currents for C and D are shown in Figures 32 through 55.

Since waveshapes A and E are very nearly the same, the induced currents from them should be also. The results are shown in Figures 56 through 79, and apparently the currents are about the same. Notice, also, that the very long "tail" of waveshape E has caused convergence problems with the numerical integration for finding the current.

Calculations for waveshape F show that the resulting currents amount to only a few amperes. This is not surprising since the frequencies involved in the electric field are microwave and the current induced in the wire from the

electric field behaves like the current in an R-L series circuit driven by a voltage source. That is, the transfer function (the ratio $I_i(\omega)/E_o(\omega)$ in equation 1) is similar to that of a simple low pass filter. This transfer function is given by $\pi a^2 \sigma \sin \theta$ for very low frequencies, while at high frequencies the magnitude falls off more slowly with frequency than -20 dB per decade ($\approx$ -18.8) and the phase is more positive than, but close to, -90 degrees. Thus, except for a larger bandwidth which results in smaller rise times, the wire itself behaves very much like a first-order low-pass filter. Based on this fact, the results are as expected. For example, the current produced by waveshape A, before the ground-reflected wave appears, is given by the approximate result

$$i_1(t) = \frac{6 \times 10^3}{(\sin \theta)^{0.9}} \exp(-90t/\sin^2\theta) \left[1 - e^{-4 \times 10^6 t}\right]$$

based on the R-L series circuit approximation. This current, as predicted, rises more slowly than the actual current.

Table 2 summarizes the results of this study for the largest currents obtained in terms of peak current in amperes per peak electric field strength in volts per meter for $\varepsilon_R = 10$, $\theta = 10°$, 36°, and 90°.

Table 2. Peak Current per Peak Electric Field (A-m/V)

Waveform	$\theta = 10°$	$\theta = 36°$	$\theta = 90°$
A,C,D,E	0.46	0.07	0.04
B	0.12	0.03	0.02

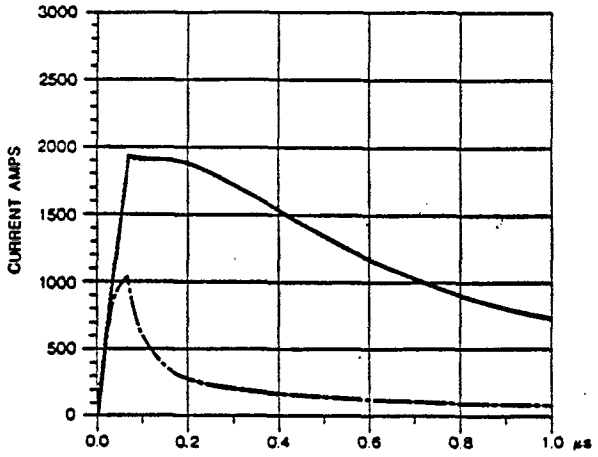

Figure 8. Current: $\theta = 90.0°$, $\sigma = 10^{-3}$, $\epsilon_R = 15$.
A ——— , C ·····, B —·—·—.

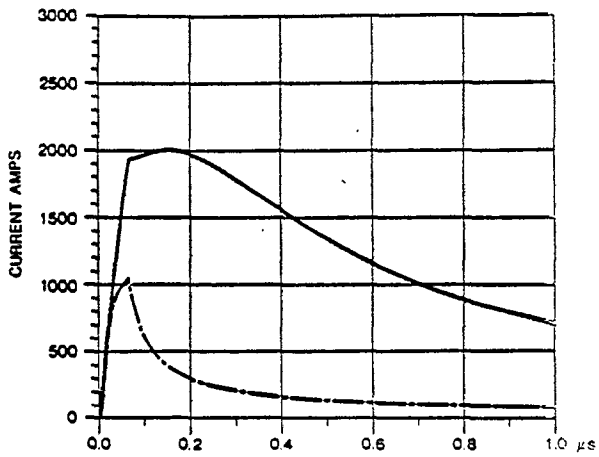

Figure 9. Current: $\theta = 90.0°$, $\sigma = 10^{-3}$, $\epsilon_R = 10$.
A ——— , C ·····, B —·—·—.

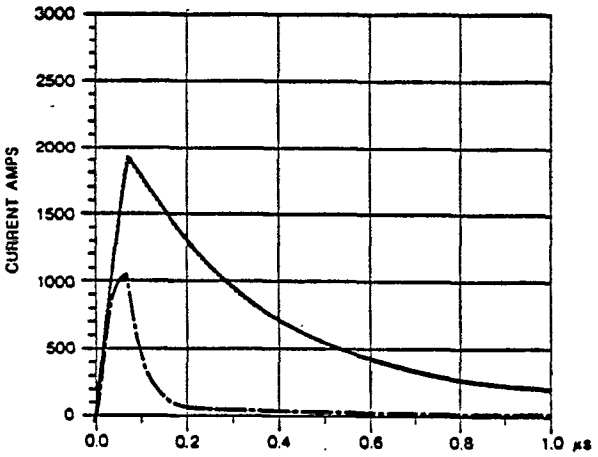

Figure 10 Current: $\theta = 90.0°$, $\sigma = 10^{-2}$, $\epsilon_R = 15$.
A ——— , C ·····, B —·—·—.

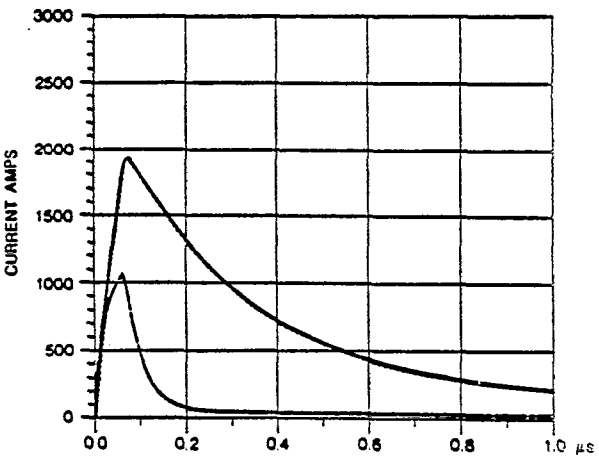

Figure 11 Current: $\theta = 90.0°$, $\sigma = 10^{-2}$, $\epsilon_R = 10$.
A ——— , C ·····, B —·—·—.

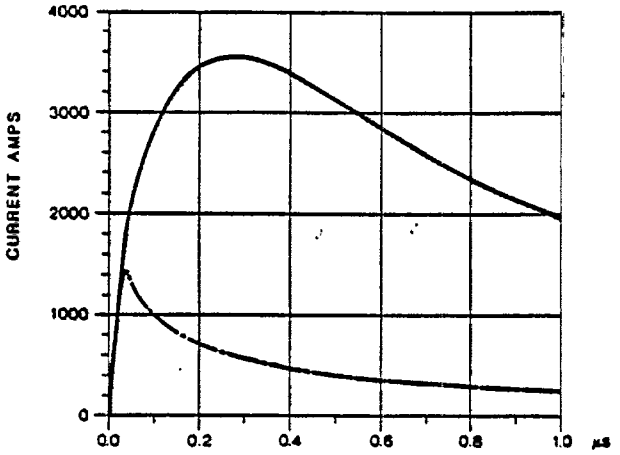

Figure 12 Current: $\theta = 36.0°$, $\sigma = 10^{-3}$, $\epsilon_R = 15$.
A ——— , C ·····, B —·—·—

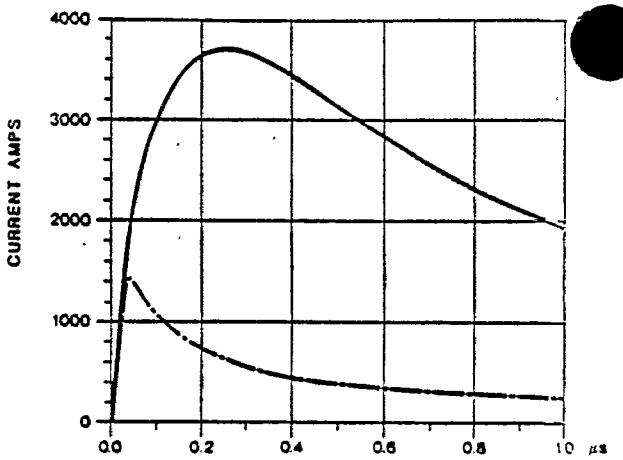

Figure 13 Current: $\theta = 36.0°$, $\sigma = 10^{-3}$, $\epsilon_R = 10$.
A ——— , C ·····, B —·—·—

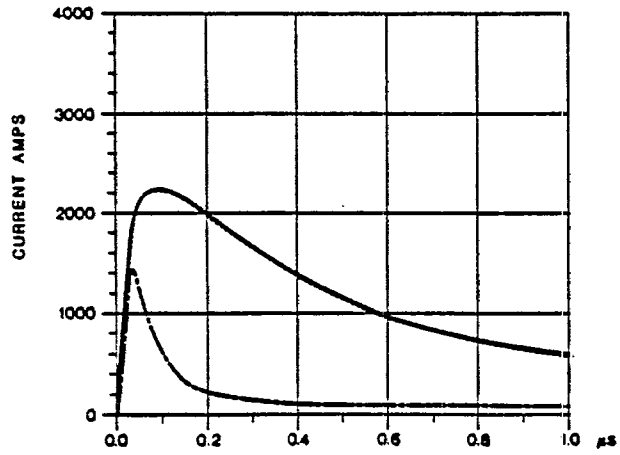

Figure 14 Current: $\theta = 36.0°$, $\sigma = 10^{-2}$, $\epsilon_R = 15$.
A ——— , C ·····, B —·—·—

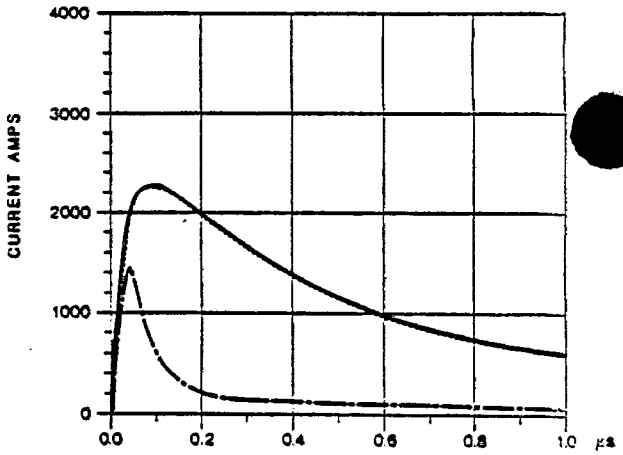

Figure 15 Current: $\theta = 36.0°$, $\sigma = 10^{-2}$, $\epsilon_R = 10$.
A ——— , C ·····, B —·—·—

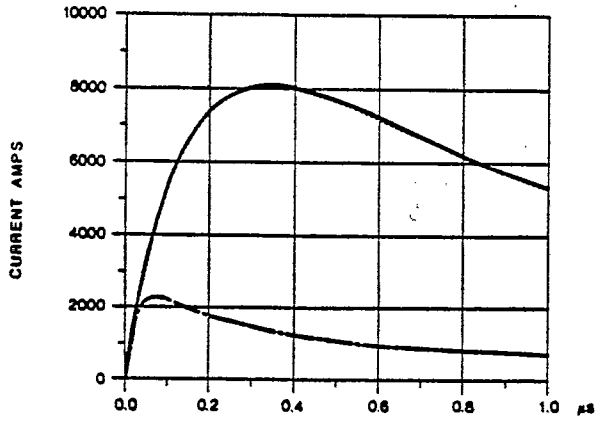

Figure 16 Current: $\theta = 20.0°$, $\sigma = 10^{-3}$, $\epsilon_R = 15$.
A ———, C ·····, B —·—·—.

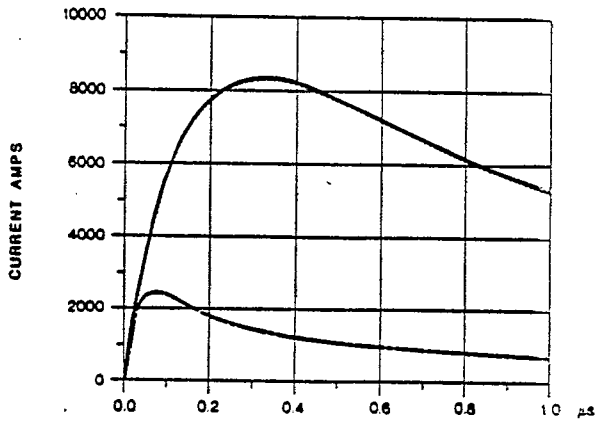

Figure 17 Current: $\theta = 20.0°$, $\sigma = 10^{-3}$, $\epsilon_R = 10$.
A ———, C ·····, B —·—·—.

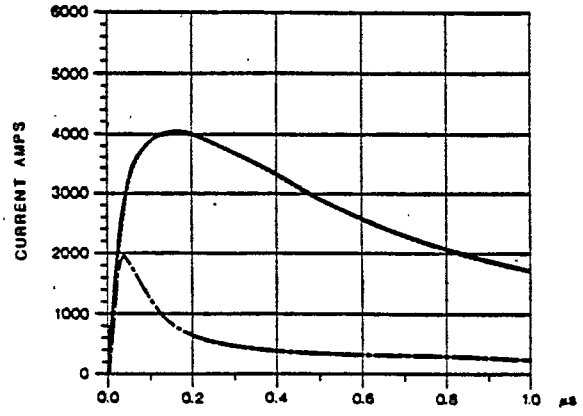

Figure 18 Current: $\theta = 20.0°$, $\sigma = 10^{-2}$, $\epsilon_R = 15$.
A ———, C ·····, B —·—·—.

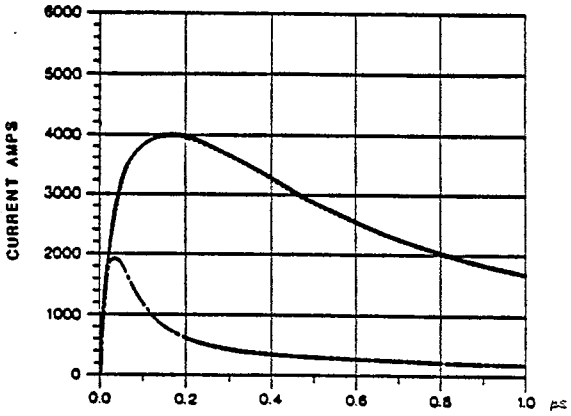

Figure 19 Current: $\theta = 20.0°$, $\sigma = 10^{-2}$, $\epsilon_R = 10$.
A ———, C ·····, B —·—·—.

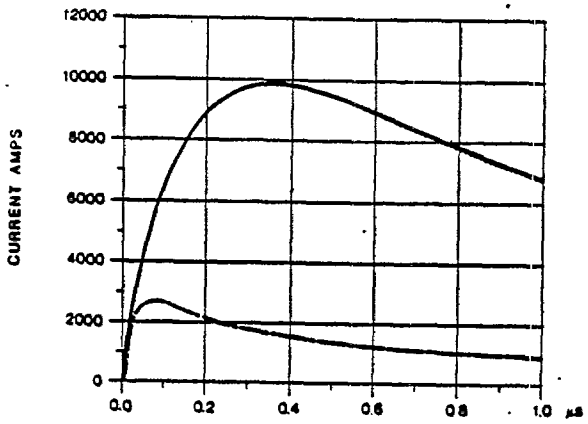

Figure 20 Current: $\theta = 17.6°$, $\sigma = 10^{-3}$, $\epsilon_R = 15$.
A ——, C - - - -, B —·—·—.

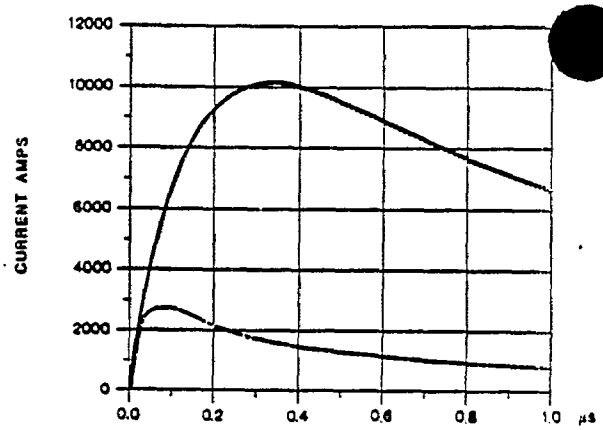

Figure 21 Current: $\theta = 17.6°$, $\sigma = 10^{-3}$, $\epsilon_R = 10$.
A ——, C - - - -, B —·—·—.

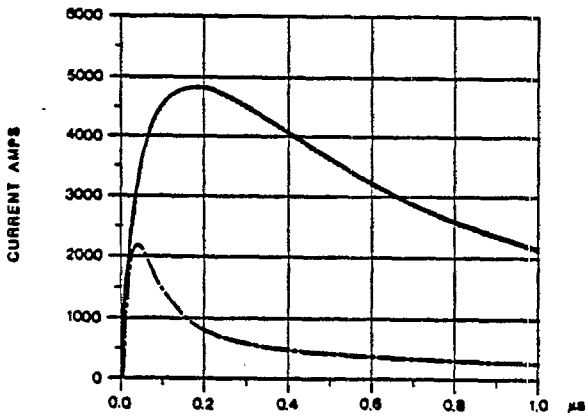

Figure 22 Current: $\theta = 17.6°$, $\sigma = 10^{-2}$, $\epsilon_R = 15$.
A ——, C - - - -, B —·—·—.

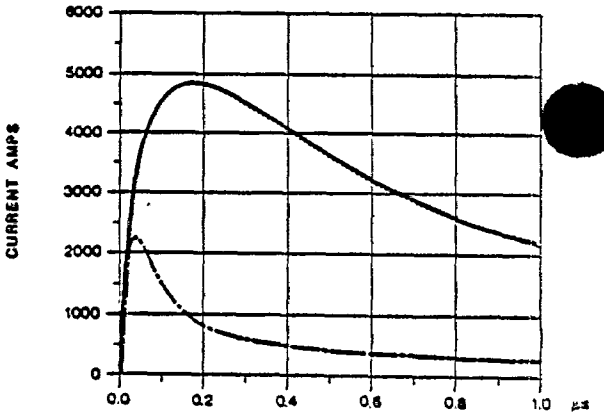

Figure 23 Current: $\theta = 17.6°$, $\sigma = 10^{-2}$, $\epsilon_R = 10$.
A ——, C - - - -, B —·—·—.

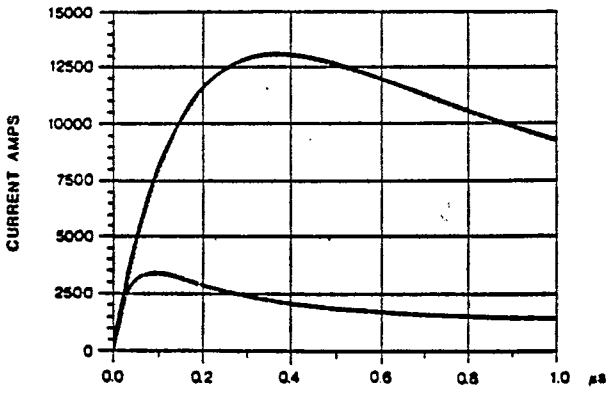

Figure 24 Current: $\theta = 14.5°$, $\sigma = 10^{-3}$, $\epsilon_R = 15$.
A ——, C ——, B ——.

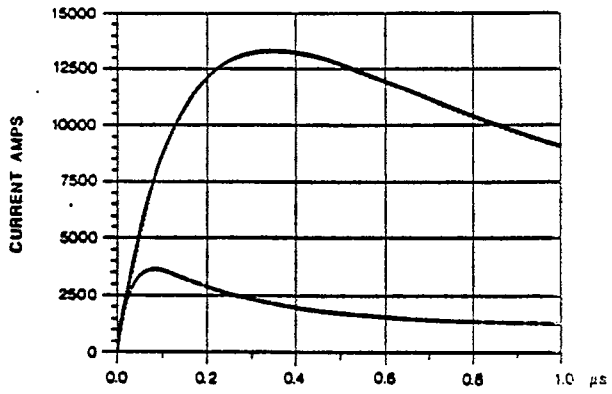

Figure 25 Current: $\theta = 14.5°$, $\sigma = 10^{-3}$, $\epsilon_R = 10$.
A ——, C ——, B ——.

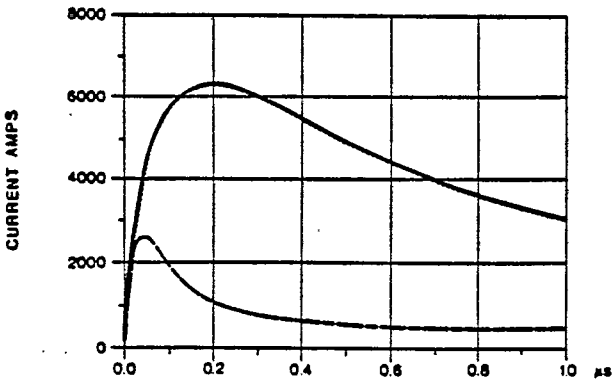

Figure 26 Current: $\theta = 14.5°$, $\sigma = 10^{-2}$, $\epsilon_R = 15$.
A ——, C ——, B ——.

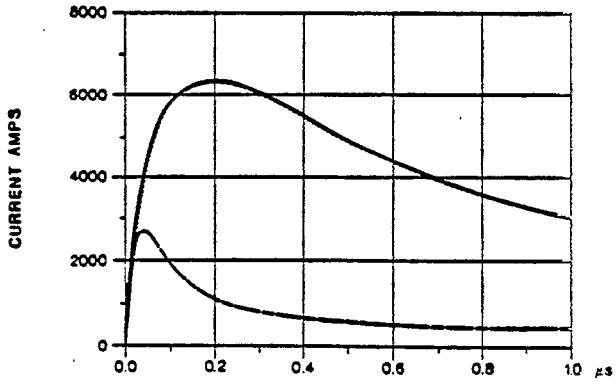

Figure 27 Current: $\theta = 14.5°$, $\sigma = 10^{-2}$, $\epsilon_R = 10$.
A ——, C ——, B ——.

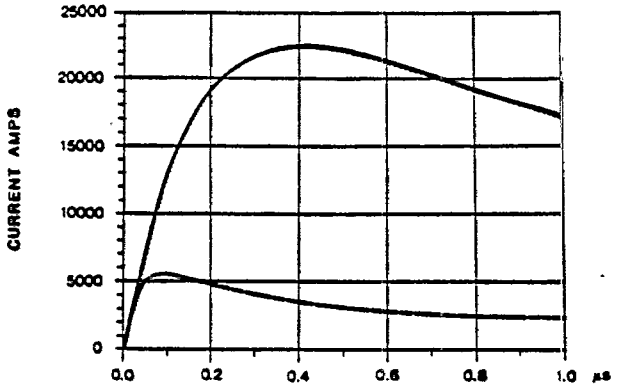

Figure 28 Current: θ=10.0°, $\sigma = 10^{-3}$, ϵ_R=15.
A———, C———, B———.

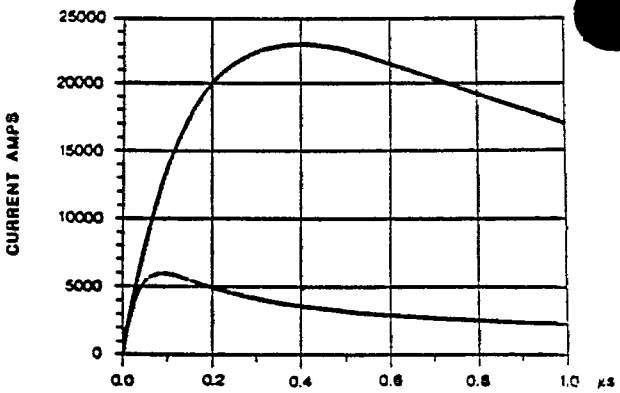

Figure 29 Current: θ=10.0°, $\sigma = 10^{-3}$, ϵ_R=10.
A———, C———, B———

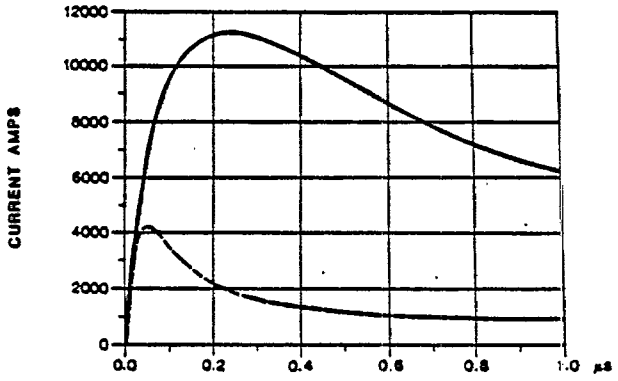

Figure 30 Current: θ=10.0°, $\sigma = 10^{-2}$, ϵ_R=15.
A———, C———, B———.

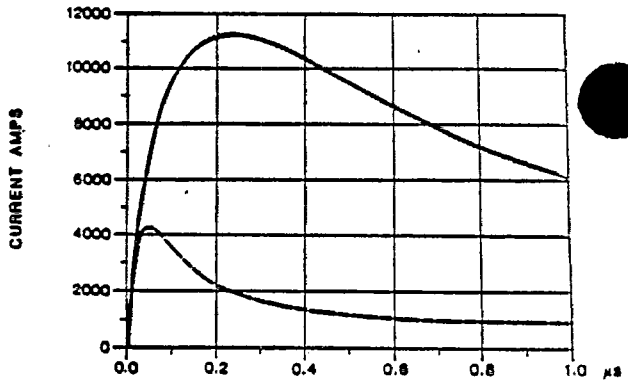

Figure 31 Current: θ=10.0°, $\sigma = 10^{-2}$, ϵ_R=10.
A———, C———, B———.

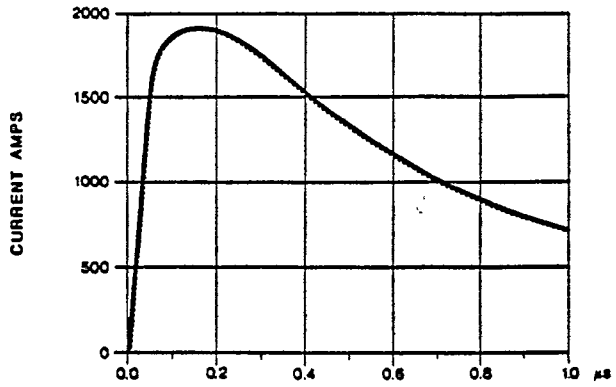

Figure 32 Current: θ=90.0°, $\sigma = 10^{-3}$, ϵ_R=15.
C ——, D ——.

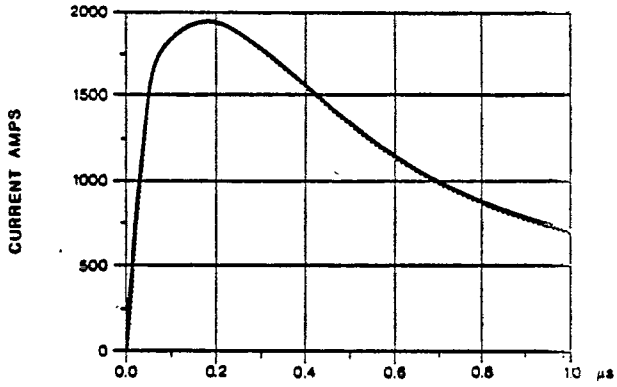

Figure 33 Current: θ=90.0°, $\sigma = 10^{-3}$, ϵ_R=10.
C ——, D ——.

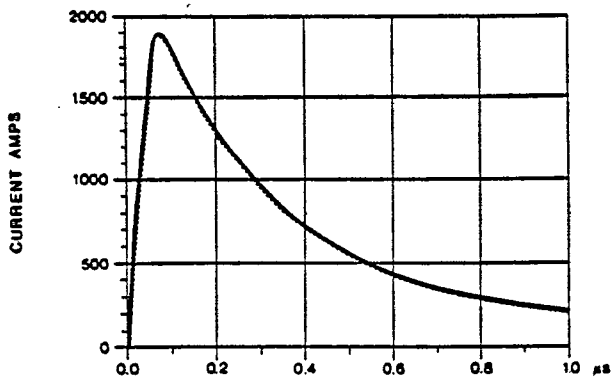

Figure 34 Current: θ=90.0°, $\sigma = 10^{-2}$, ϵ_R=15.
C ——, D ——.

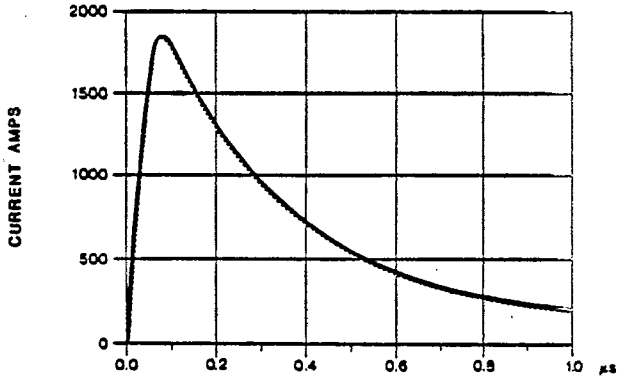

Figure 35 Current: θ=90.0°, $\sigma = 10^{-2}$, ϵ_R=10.
C ——, D ——.

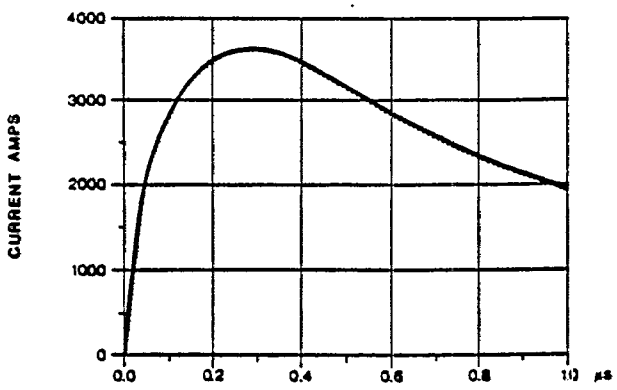

Figure 36 Current: θ=36.0°, $\sigma = 10^{-3}$, ϵ_R=15.
C ——————, D ——————.

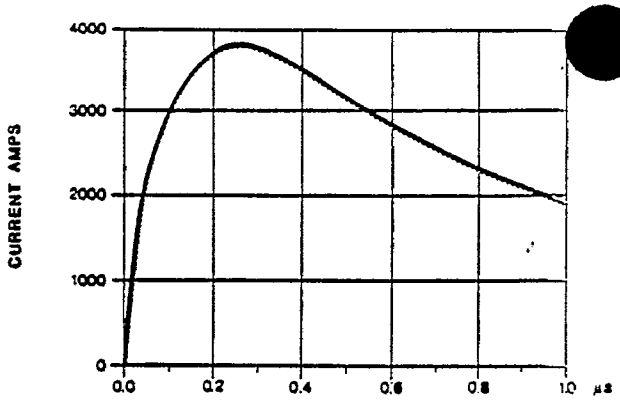

Figure 37 Current: θ=36.0°, $\sigma = 10^{-3}$, ϵ_R=10.
C ——————, D ——————.

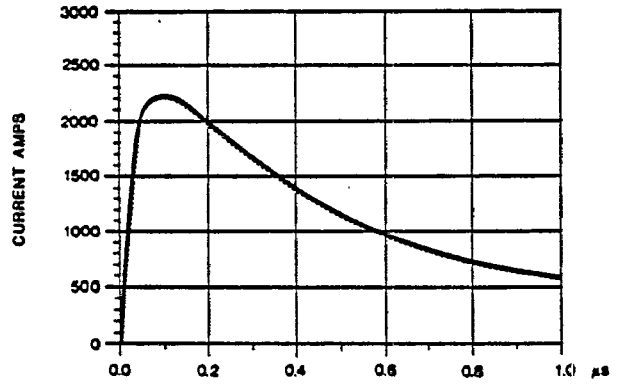

Figure 38 Current: θ=36.0°, $\sigma = 10^{-2}$, ϵ_R=15.
C ——————, D ——————.

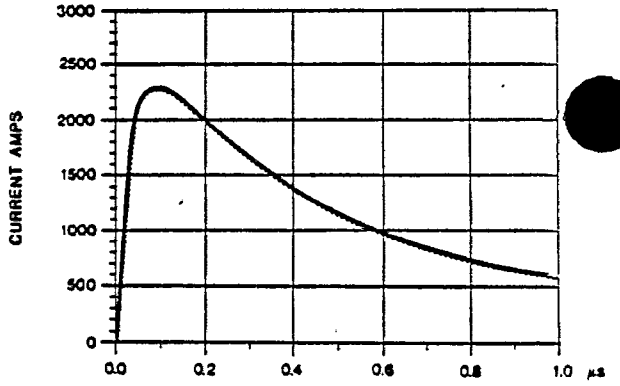

Figure 39 Current: θ=36.0, $\sigma = 10^{-2}$, ϵ_R=10.
C ——————, D ——————.

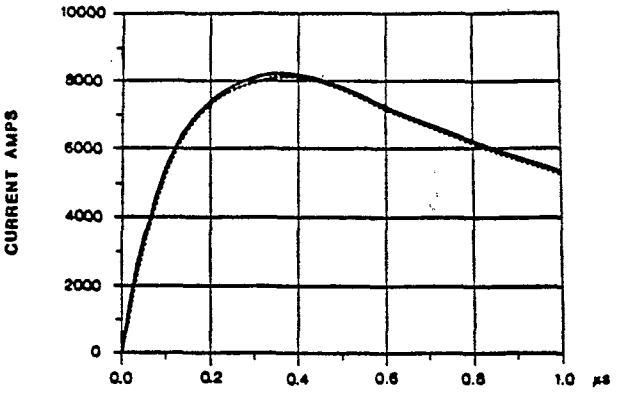

Figure 40 Current: θ=20.0°, $\sigma = 10^{-3}$, ϵ_R=15.
C ——, D ——.

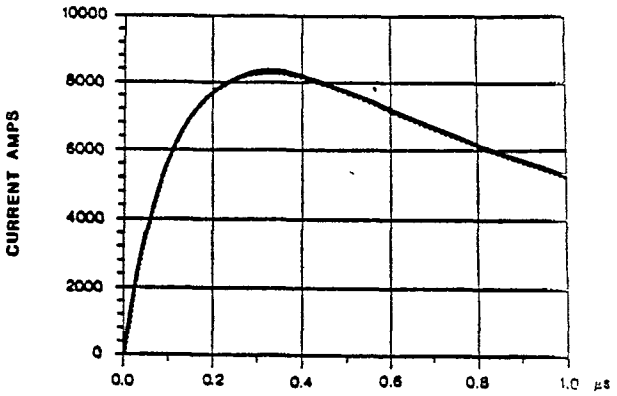

Figure 41 Current: θ=20.0°, $\sigma = 10^{-3}$, ϵ_R=10.
C ——, D ——.

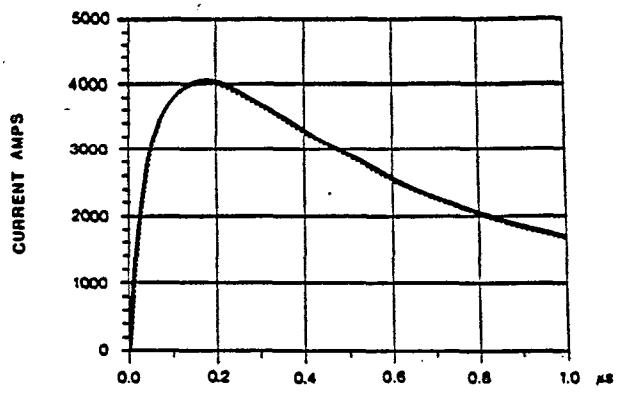

Figure 42 Current: θ=20.0°, $\sigma = 10^{-2}$, ϵ_R=15.
C ——, D ——.

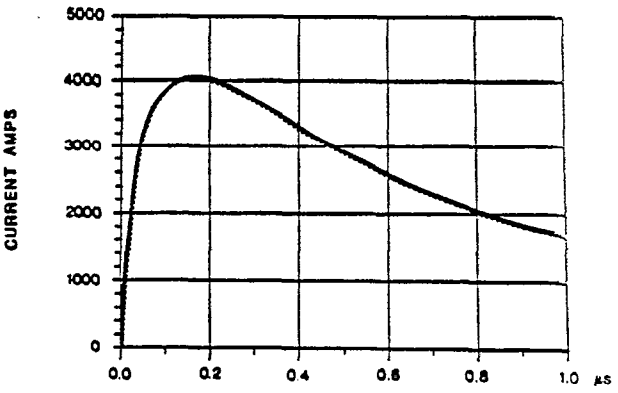

Figure 43 Current: θ=20.0°, $\sigma = 10^{-2}$, ϵ_R=10.
C ——, D ——.

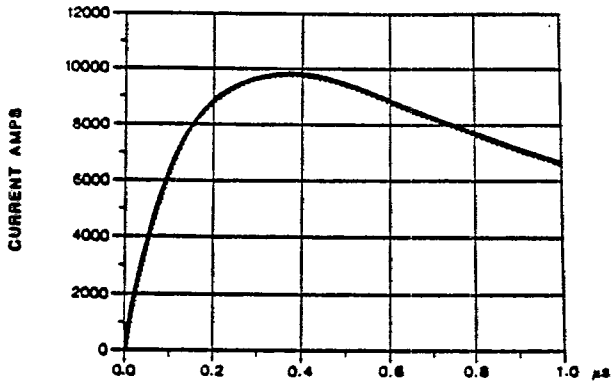

Figure 44 Current: $\theta = 17.6°$, $\sigma = 10^{-3}$, $\epsilon_R = 15$.
C ———, D ———.

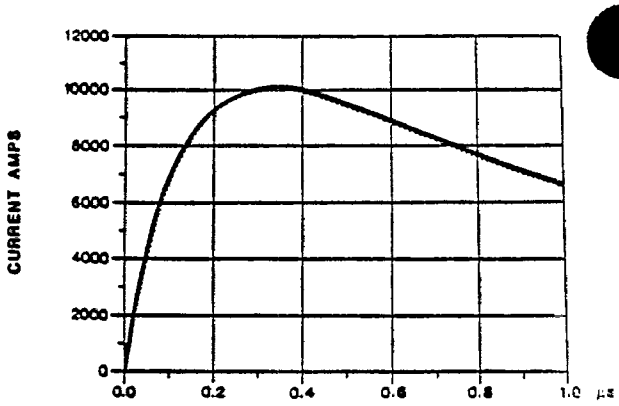

Figure 45 Current: $\theta = 17.6°$, $\sigma = 10^{-3}$, $\epsilon_R = 10$.
C ———, D ———.

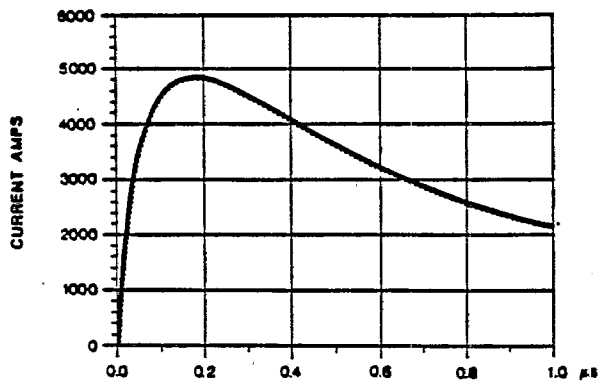

Figure 46 Current: $\theta = 17.6°$, $\sigma = 10^{-2}$, $\epsilon_R = 15$.
C ———, D ———.

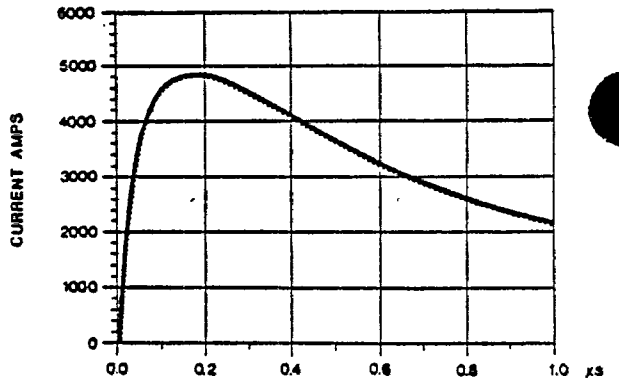

Figure 47 Current: $\theta = 17.6°$, $\sigma = 10^{-2}$, $\epsilon_R = 10$.
C ———, D ———.

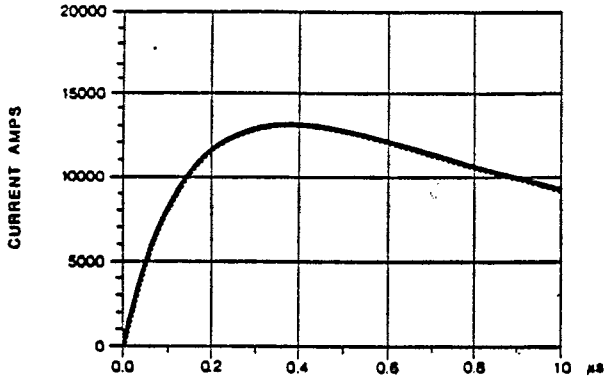

Figure 48 Current: $\theta = 14.5°$, $\sigma = 10^{-3}$, $\epsilon_R = 15$.
C ——————, D ——————.

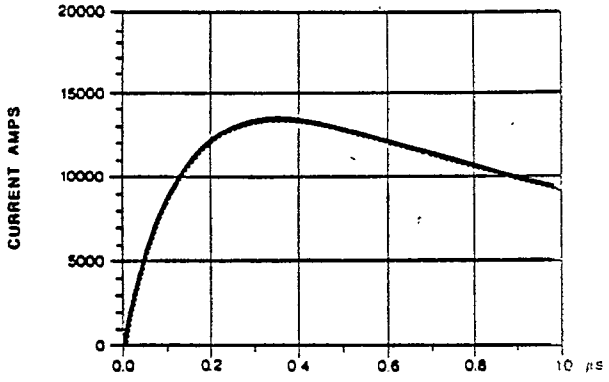

Figure 49 Current: $\theta = 14.5°$, $\sigma = 10^{-3}$, $\epsilon_R = 10$.
C ——————, D ——————.

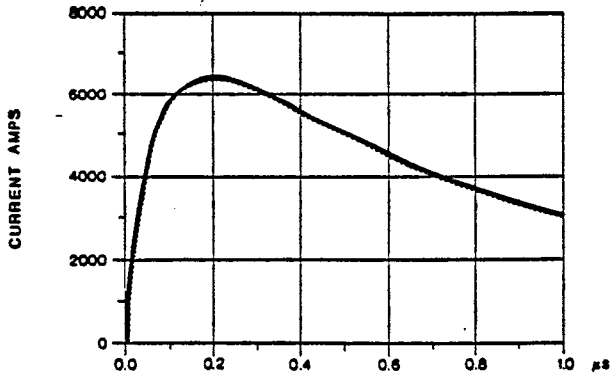

Figure 50 Current: $\theta = 14.5°$, $\sigma = 10^{-2}$, $\epsilon_R = 15$.
C ——————, D ——————.

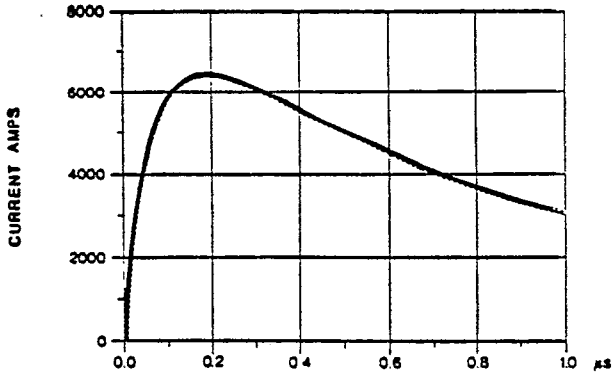

Figure 51 Current: $\theta = 14.5°$, $\sigma = 10^{-2}$, $\epsilon_R = 10$.
C ——————, D ——————.

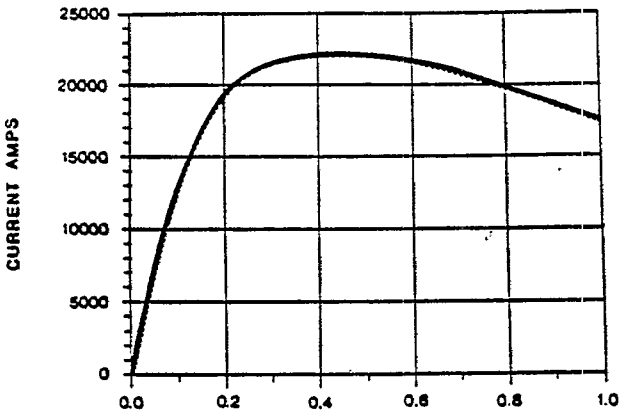

Figure 52 Current: $\theta = 10.0°$, $\sigma = 10^{-3}$, $\epsilon_R = 15$.
C ——————, D ----------.

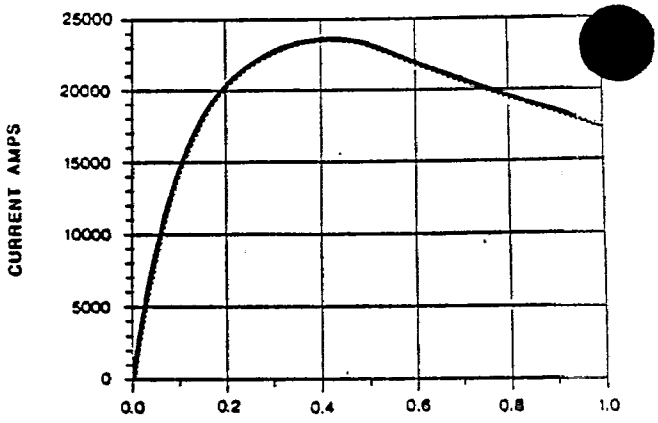

Figure 53 Current: $\theta = 10.0°$, $\sigma = 10^{-3}$, $\epsilon_R = 10$.
C ——————, D ----------.

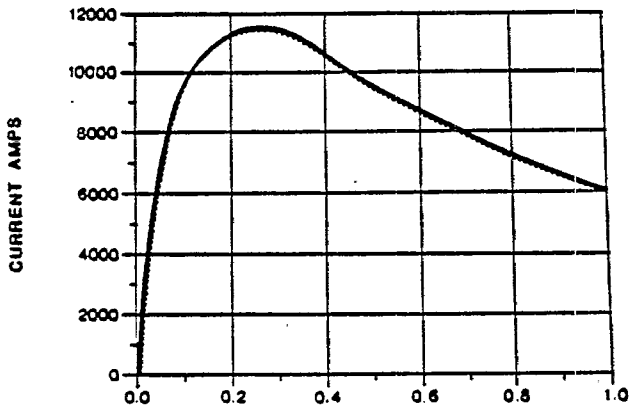

Figure 54 Current: $\theta = 10.0°$, $\sigma = 10^{-2}$, $\epsilon_R = 15$.
C ——————, D ----------.

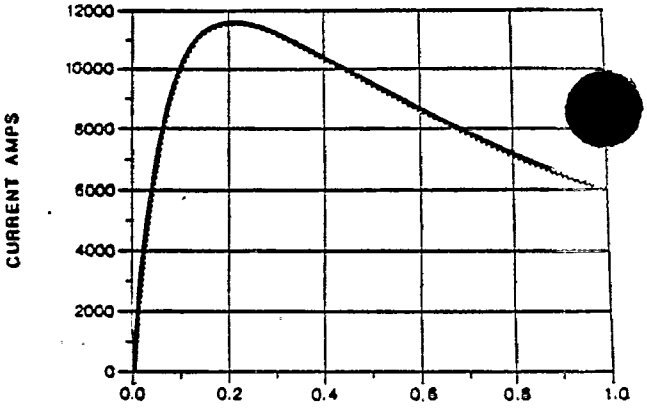

Figure 55 Current: $\theta = 10.0°$, $\sigma = 10^{-2}$, $\epsilon_R = 10$.
C ——————, D ----------.

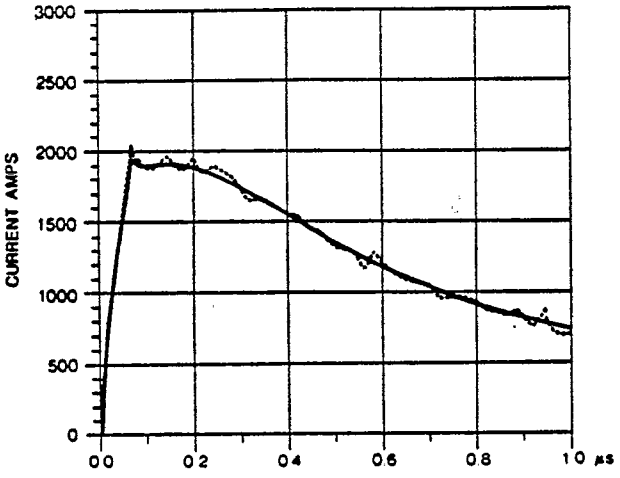

Figure 56 Current: $\theta = 90.0°$, $\sigma = 10^{-3}$, $\epsilon_R = 15$.
A ——, E ·····.

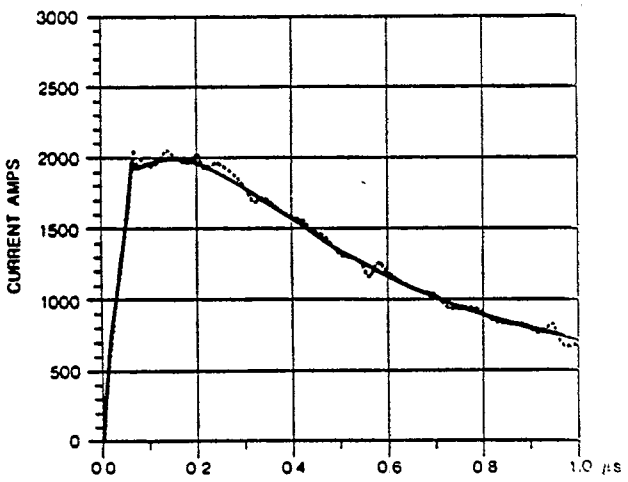

Figure 57 Current: $\theta = 90.0°$, $\sigma = 10^{-3}$, $\epsilon_R = 10$.
A ——, E ·····.

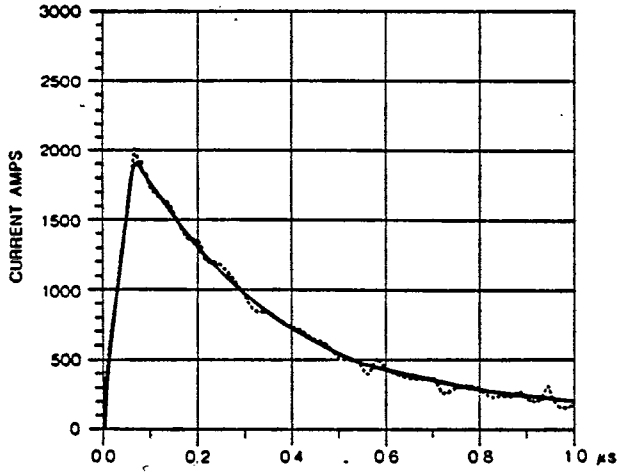

Figure 58 Current: $\theta = 90.0°$, $\sigma = 10^{-2}$, $\epsilon_R = 15$.
A ——, E ·····.

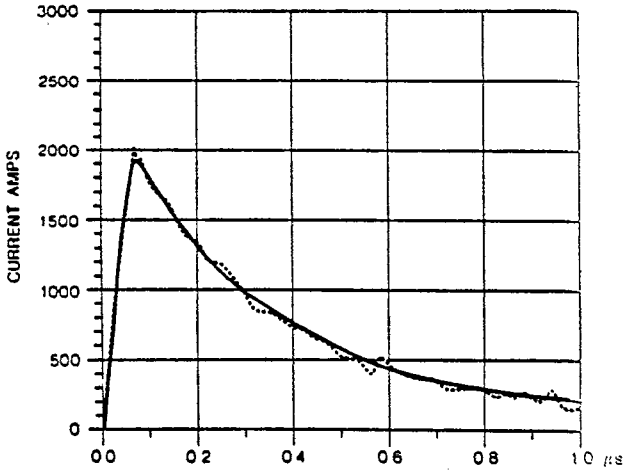

Figure 59 Current: $\theta = 90.0°$, $\sigma = 10^{-2}$, $\epsilon_R = 10$.
A ——, E ·····.

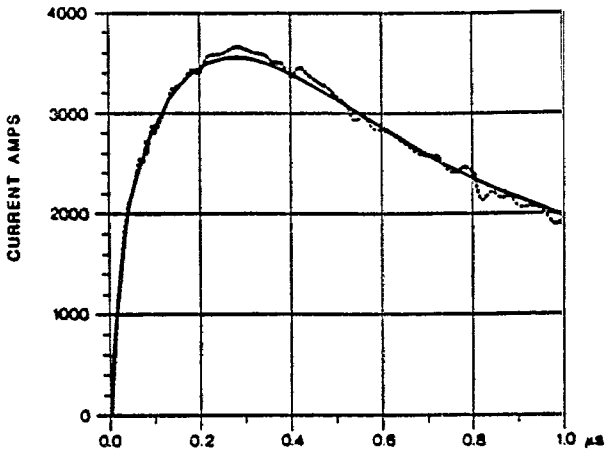

Figure 60 Current: $\theta = 36.0°$, $\sigma = 10^{-3}$, $\epsilon_R = 15$.
A ——— , E ——— .

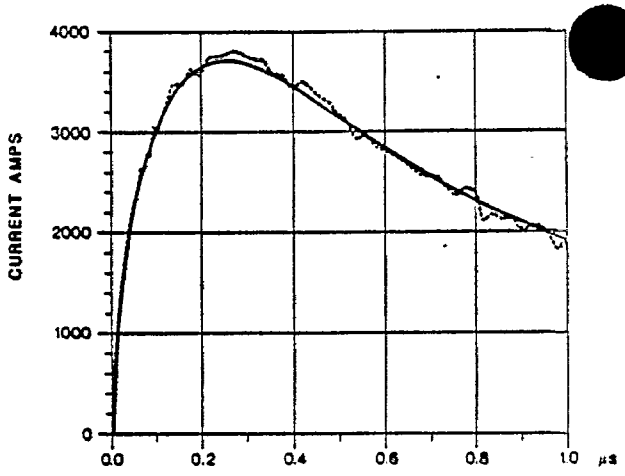

Figure 61 Current: $\theta = 36.0°$, $\sigma = 10^{-3}$, $\epsilon_R = 10$.
A ——— , E ——— .

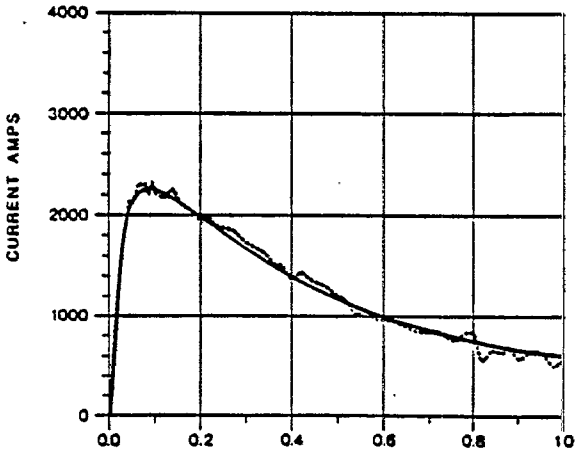

Figure 62 Current: $\theta = 36.0°$, $\sigma = 10^{-2}$, $\epsilon_R = 15$.
A ——— , E ——— .

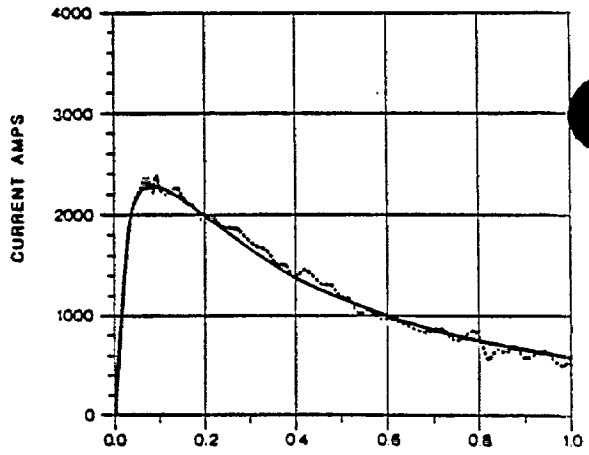

Figure 63 Current: $\theta = 36.0°$, $\sigma = 10^{-2}$, $\epsilon_R = 10$.
A ——— , E ——— .

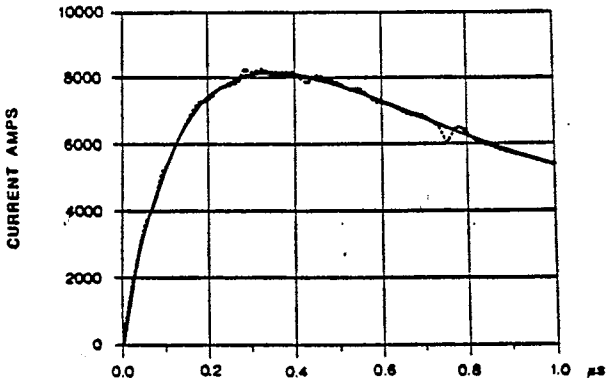

Figure 64 Current: θ=20.0°, $\sigma = 10^{-3}$, ϵ_R=15.
A ——————, E ——————.

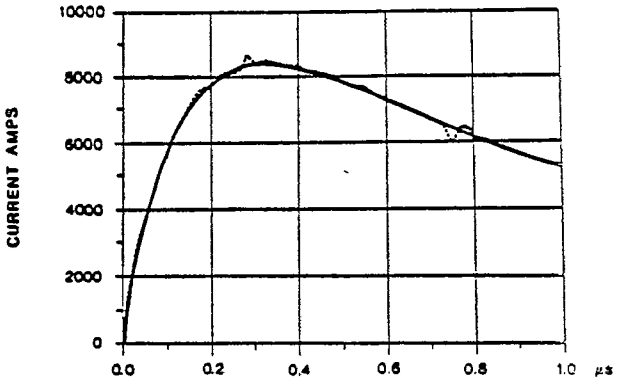

Figure 65 Current: θ=20.0°, $\sigma = 10^{-3}$, ϵ_R=10.
A ——————, E ——————.

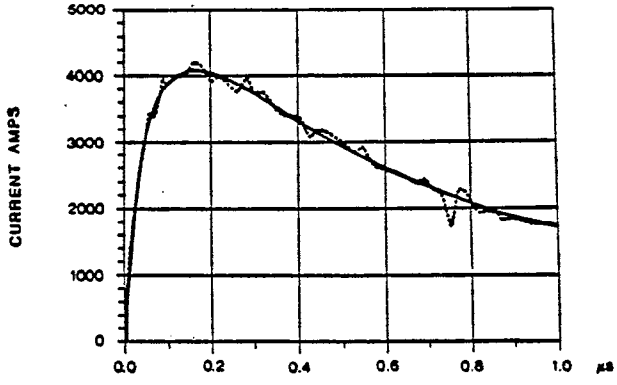

Figure 66 Current: θ=20.0°, $\sigma = 10^{-2}$, ϵ_R=15.
A ——————, E ——————.

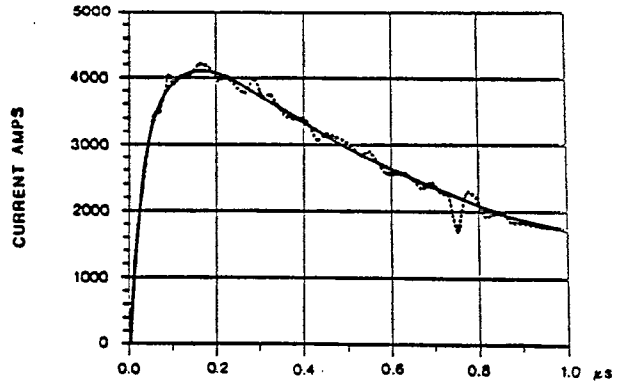

Figure 67 Current: θ=20.0°, $\sigma = 10^{-2}$, ϵ_R=10.
A ——————, E ——————.

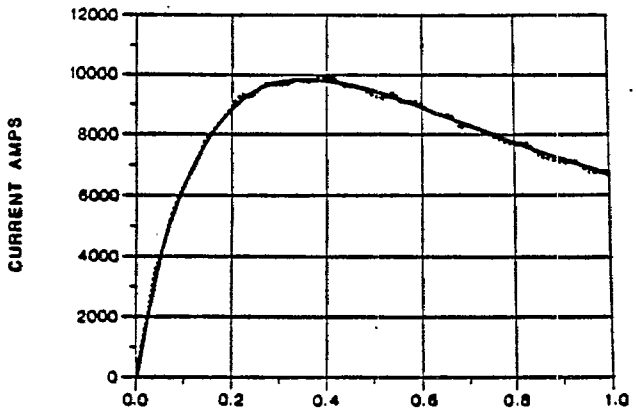

Figure 68 Current: θ=17.6°, $\sigma = 10^{-3}$, ϵ_R=15.
A———, E ———.

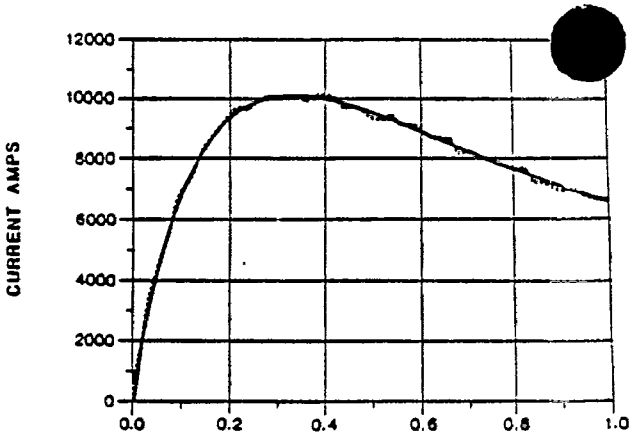

Figure 69 Current: θ=17.6°, $\sigma = 10^{-3}$, ϵ_R=10.
A———, E ———.

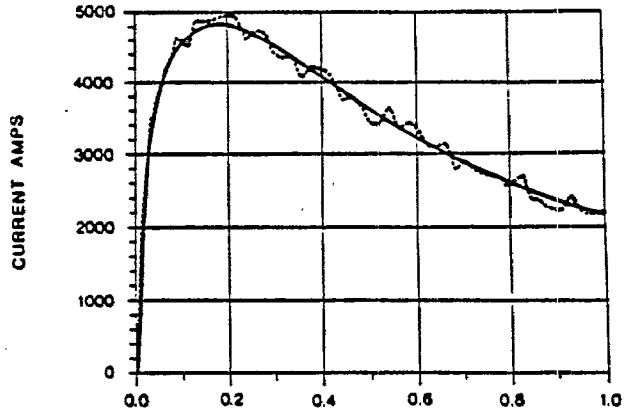

Figure 70 Current: θ=17.6°, $\sigma = 10^{-2}$, ϵ_R=15.
A———, E ———.

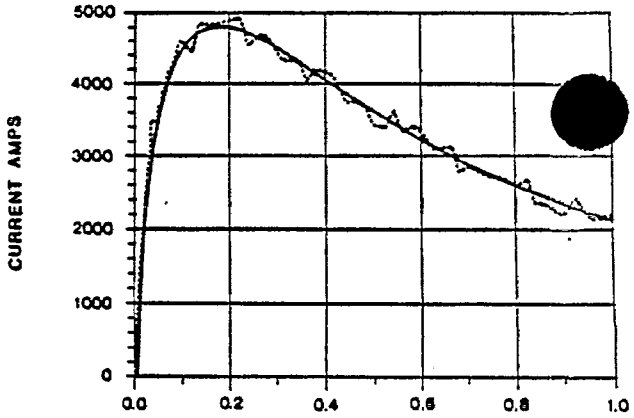

Figure 71 Current: θ=17.6°, $\sigma = 10^{-2}$, ϵ_R=10.
A———, E ———.

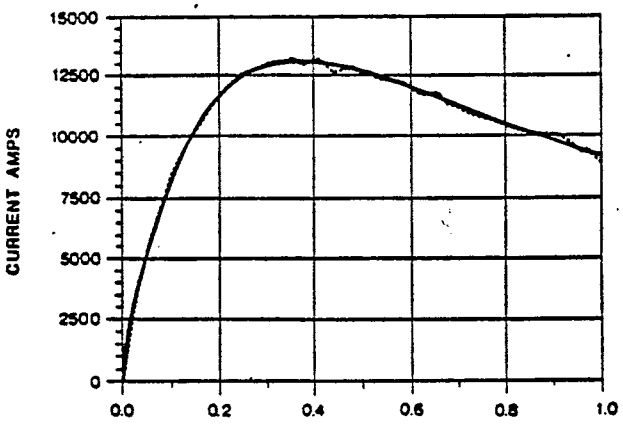

Figure 72 Current: $\theta = 14.5^{\circ}$, $\sigma = 10^{-3}$, $\epsilon_R = 15$.
A ——, E ——.

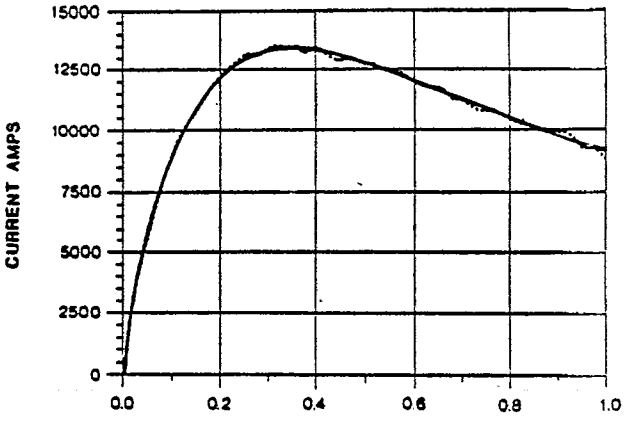

Figure 73 Current: $\theta = 14.5^{\circ}$, $\sigma = 10^{-3}$, $\epsilon_R = 10$.
A ——, E ——.

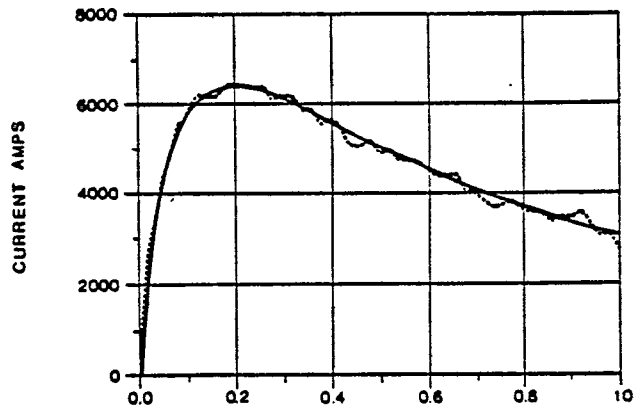

Figure 74 Current: $\theta = 14.5^{\circ}$, $\sigma = 10^{-2}$, $\epsilon_R = 15$.
A ——, E ——.

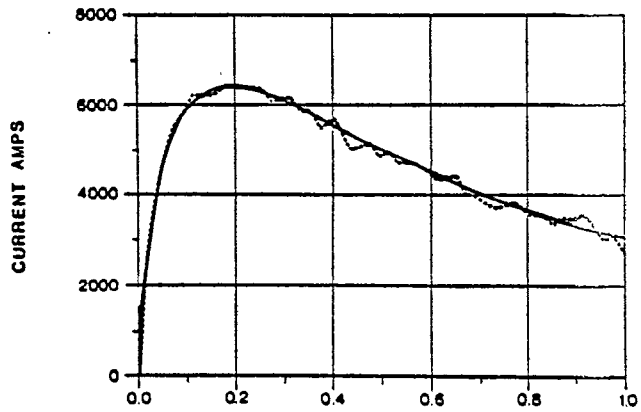

Figure 75 Current: $\theta = 14.5^{\circ}$, $\sigma = 10^{-2}$, $\epsilon_R = 10$.
A ——, E ——.

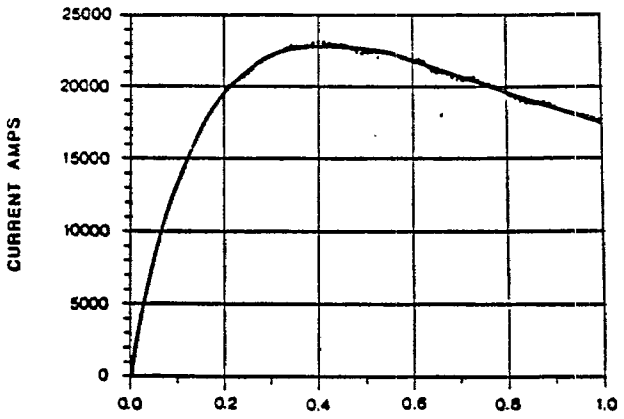

Figure 76 Current: θ=10.0°, $\sigma = 10^{-3}$, ϵ_R=15.
A ——————, E ----------.

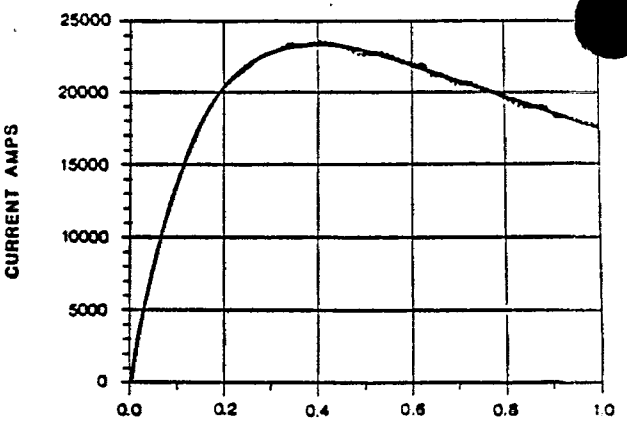

Figure 77 Current: θ=10.0°, $\sigma = 10^{-3}$, ϵ_R=10.
A ——————, E ----------.

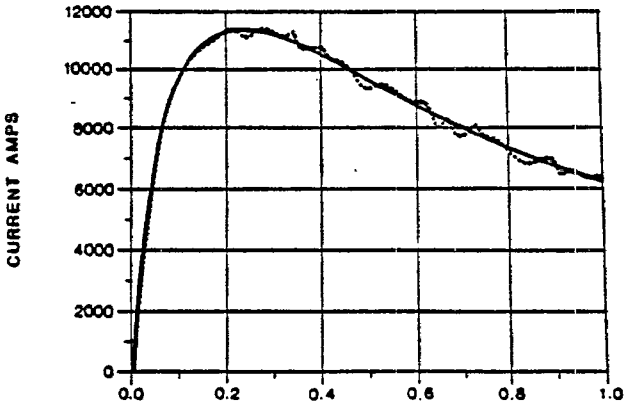

Figure 78 Current: θ=10.0°, $\sigma = 10^{-2}$, ϵ_R=15.
A ——————, E ----------.

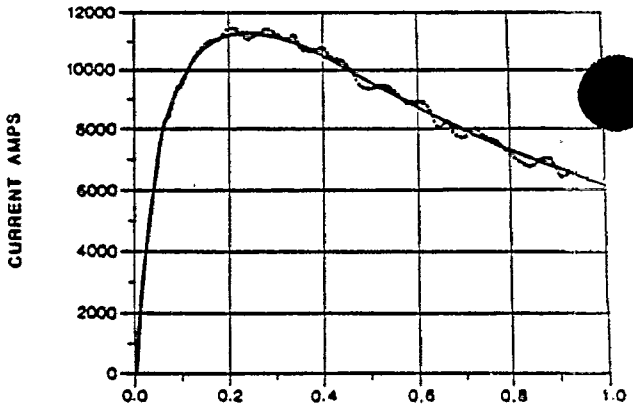

Figure 79 Current: θ=10.0°, $\sigma = 10^{-2}$, ϵ_R=10
A ——————, E ----------.

V. CONCLUDING REMARKS

Electric fields that possess very small rise times and relatively large fall times induce currents in infinitely long wires that depend almost entirely on the fall time when the effect of the ground is ignored. The ground-reflected wave reduces the peak current induced in the wire by an amount that depends strongly on θ and ε_R, the peak current being larger for smaller values of θ and larger for larger values of ε_R. The peak current, generally speaking, is reduced to roughly one-half what it would be without the ground reflection.

REFERENCES

1. H. P. Neff, Jr. and D. A. Reed, "Finitely Conducting, Infinitely Long, Cylindrical Wire in the Presence of a Plane Wave (EMP)", IN 436, February 1984.
2. H. P. Neff, Jr. and D. A. Reed, "Multiple Parallel Wires above a Finitely Conducting Plane Earth in the Presence of Plane Wave (EMP", Progress Report, ORNL, 1984.
3. H. P. Neff, Jr. and D. A. Reed, "Plane Wave (EMP) Incidence on a Finitely Conducting Plane Earth with the Magnetic Field Intensity Parallel to the Earth's Surface", TN 351, February, 1984.
4. C. E. Baum, "The Reflection of Pulsed Waves from the Surface of a Conducting Dielectric," Theoretical Notes, TN25, AFWL, Kirtland AFB, NM, February, 1967.

APPENDIX A

Figures A.1-A.5: $E_0(\omega)$ [Fourier transform of $e_0(t)$: magnitude in dB, angle in degrees] versus ω.

Figures A.6-A.13: $\Gamma_H(\omega)$ versus ω (magnitude in dB, angle in degrees).

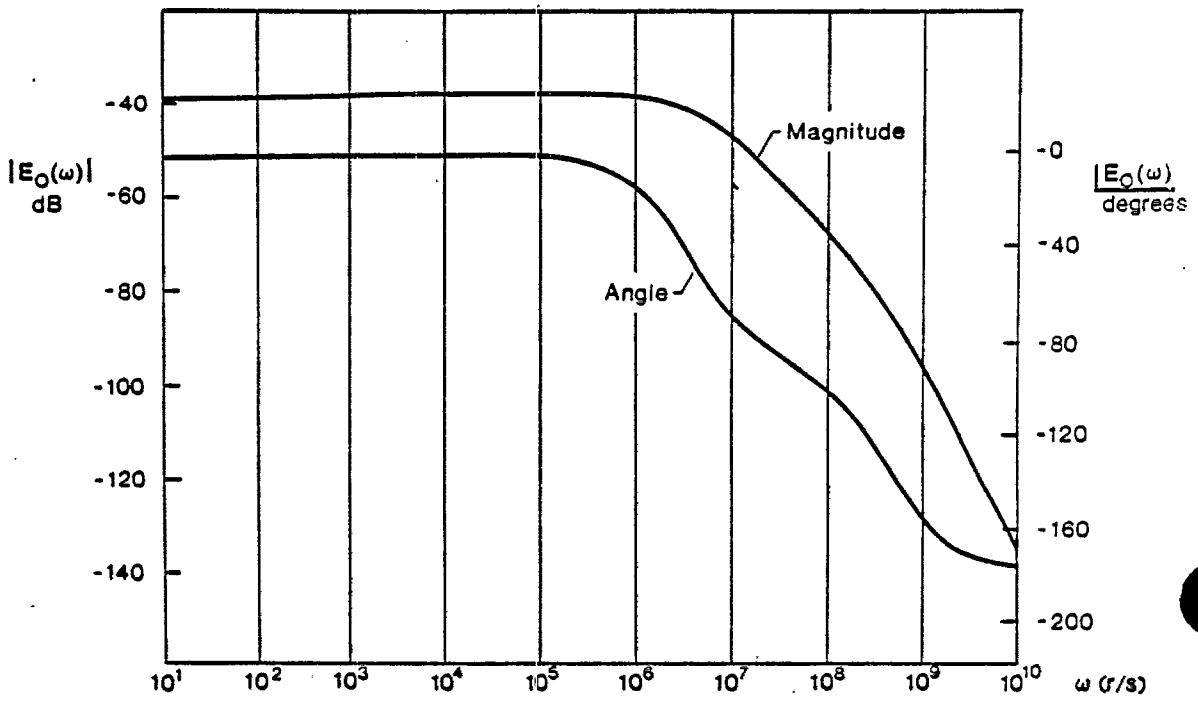
|E_O(ω)|
dB
-40
-60
-80
-100
-120
-140
Magnitude
Angle
-0
-40
-80
-120
-160
-200
∠E_O(ω)
degrees
10^1
10^2
10^3
10^4
10^5
10^6
10^7
10^8
10^9
10^10
ω (r/s)

Figure A.1 A.

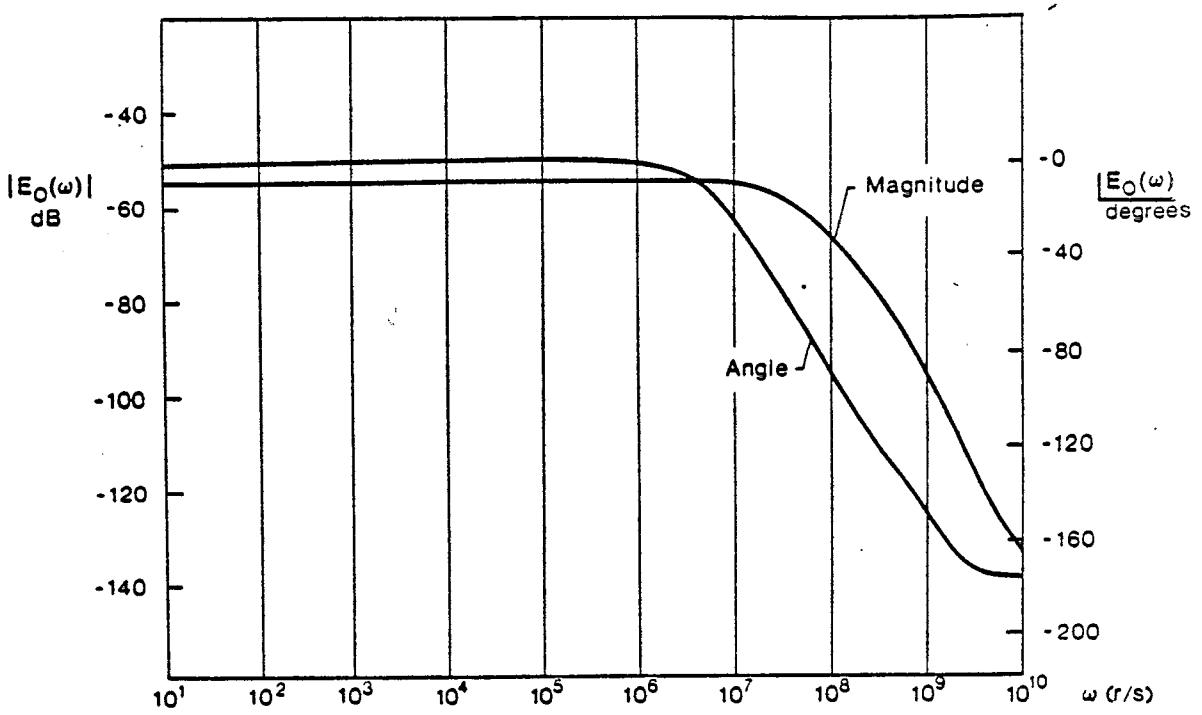

Figure A.2 B.

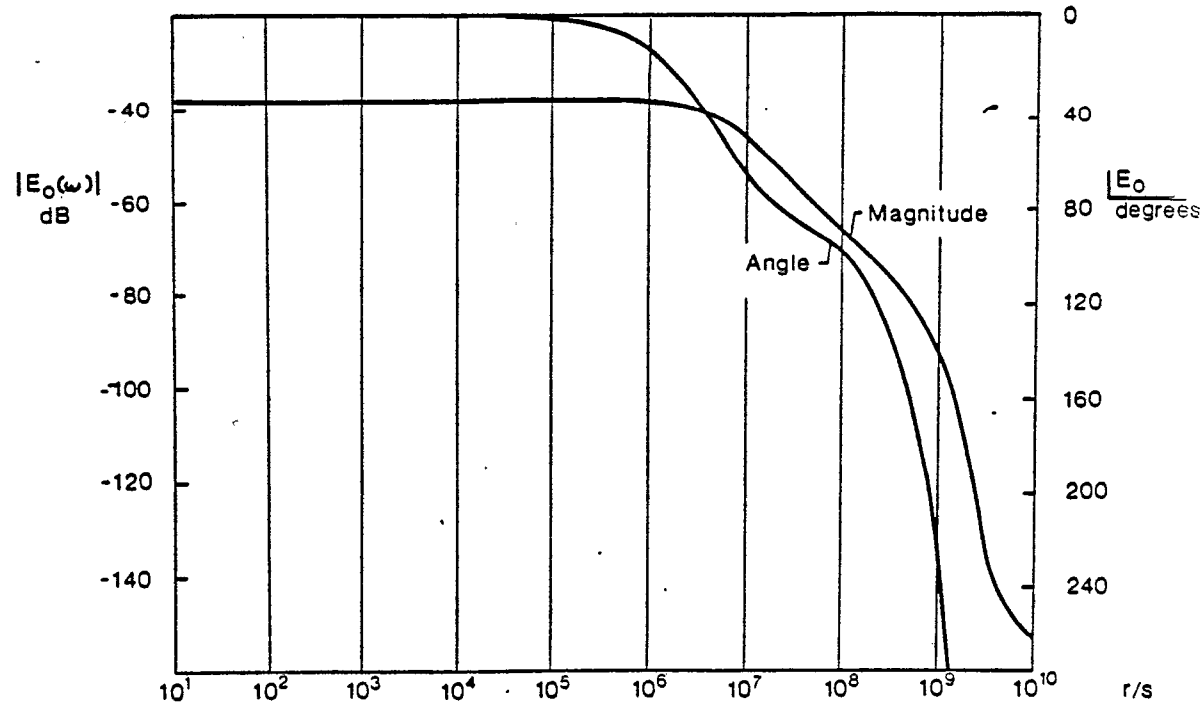

Figure A.3 C.

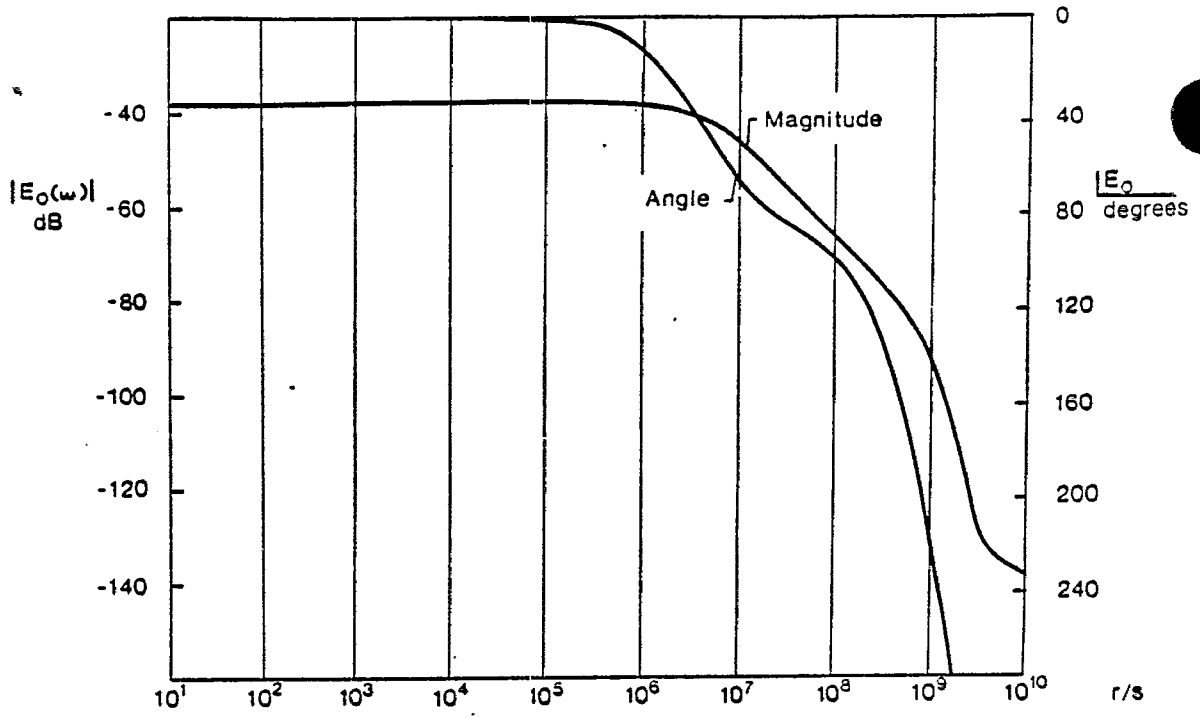

Figure A.4 D.

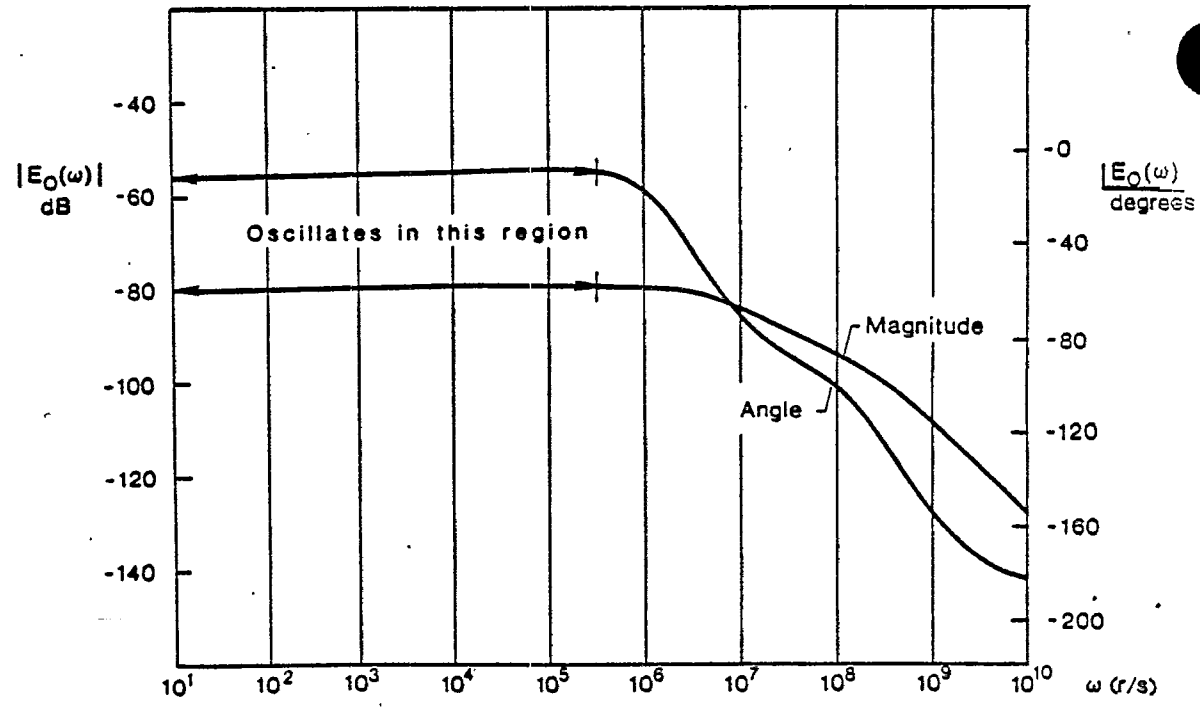

Figure A.5 E.

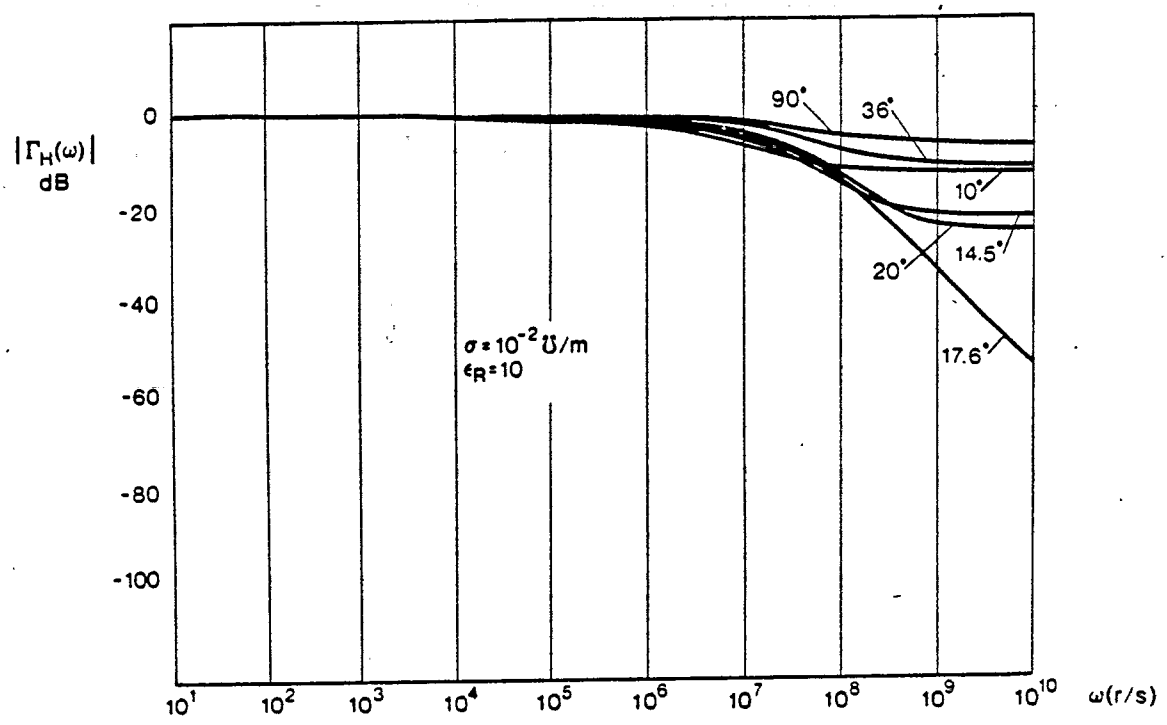

Figure A.6.

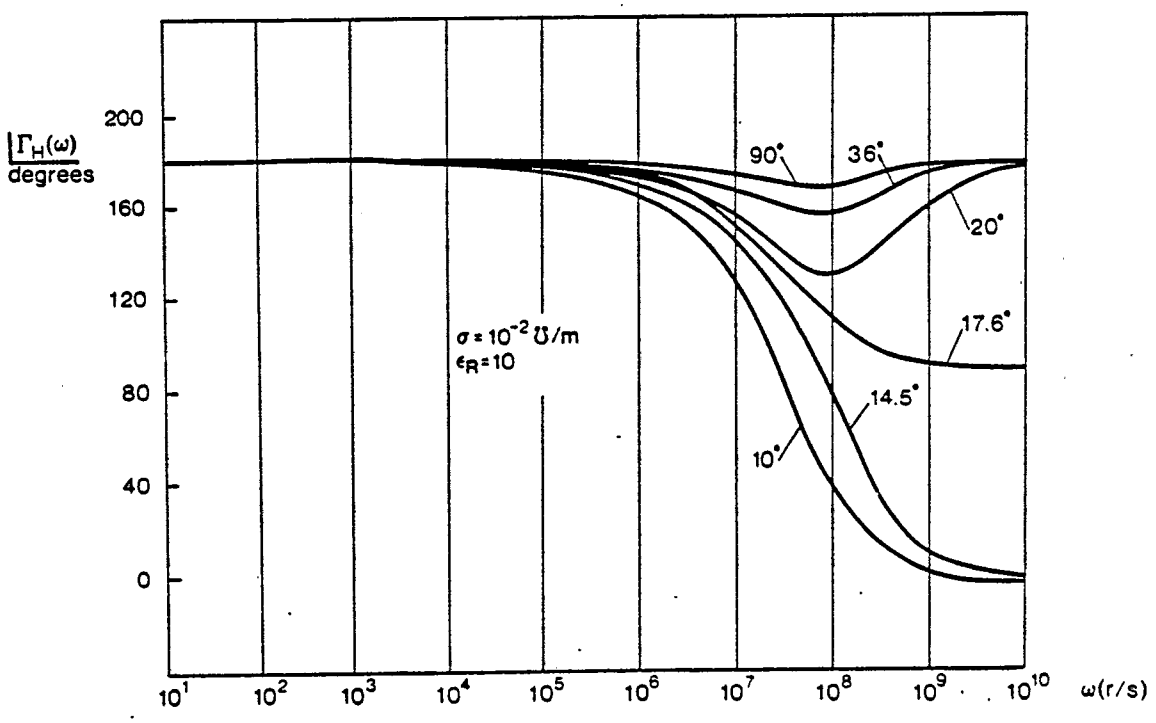

Figure A.7.

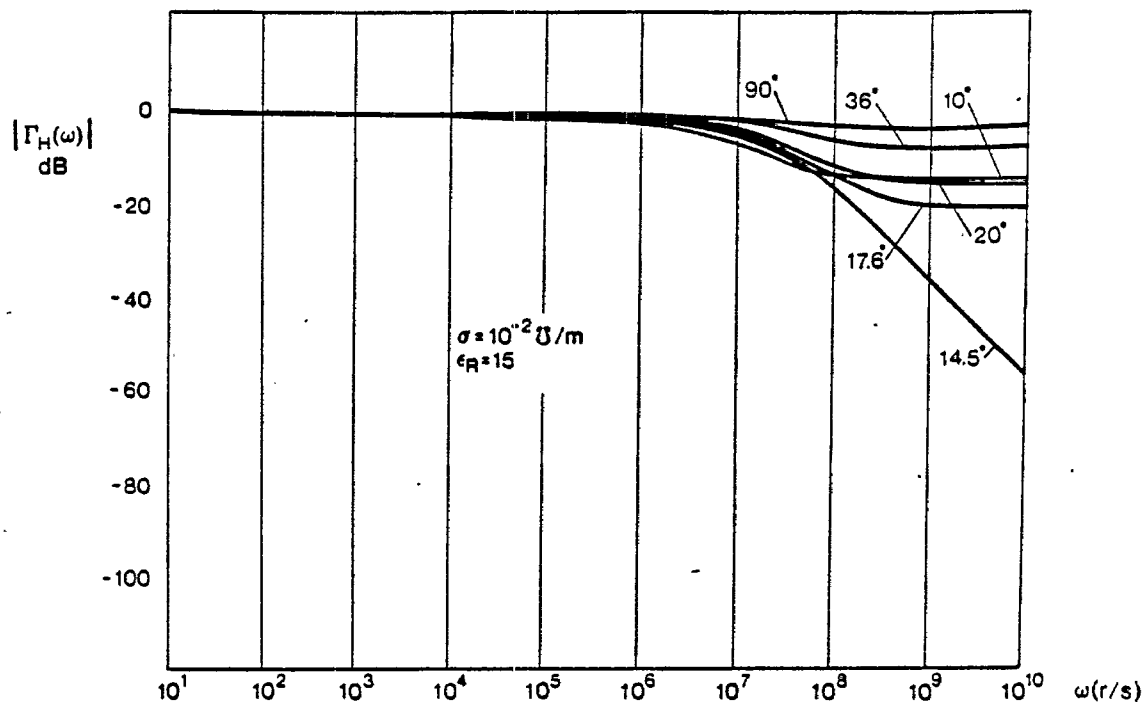

Figure A. 8 .

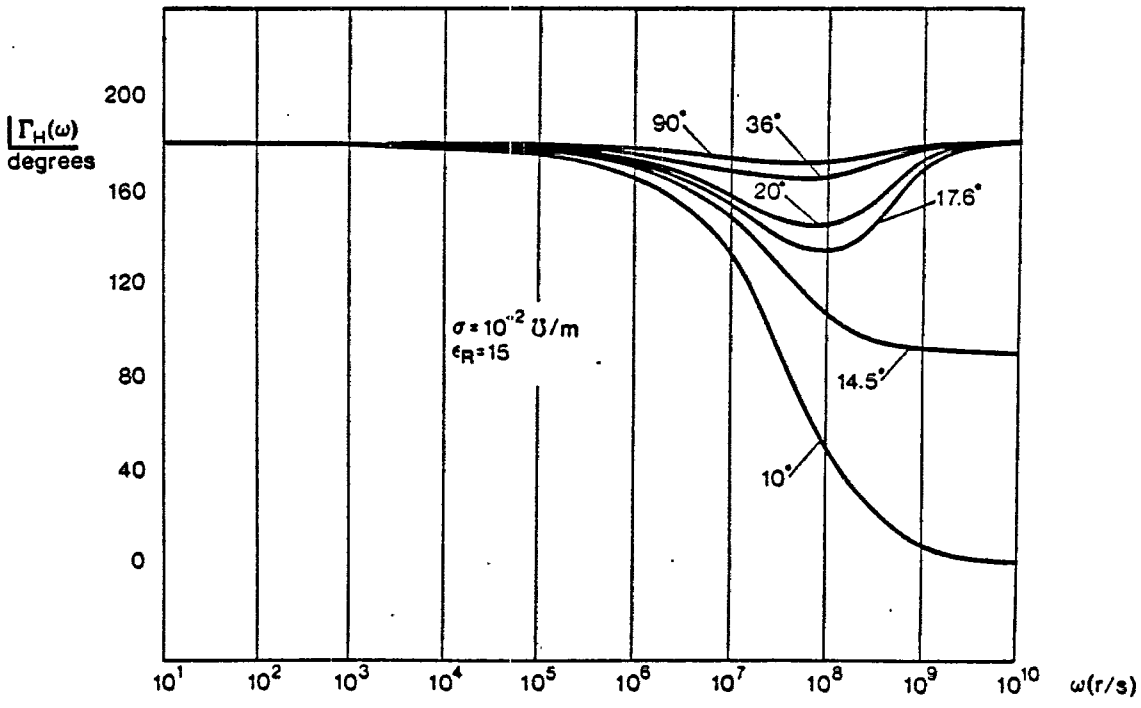

Figure A. 9 .

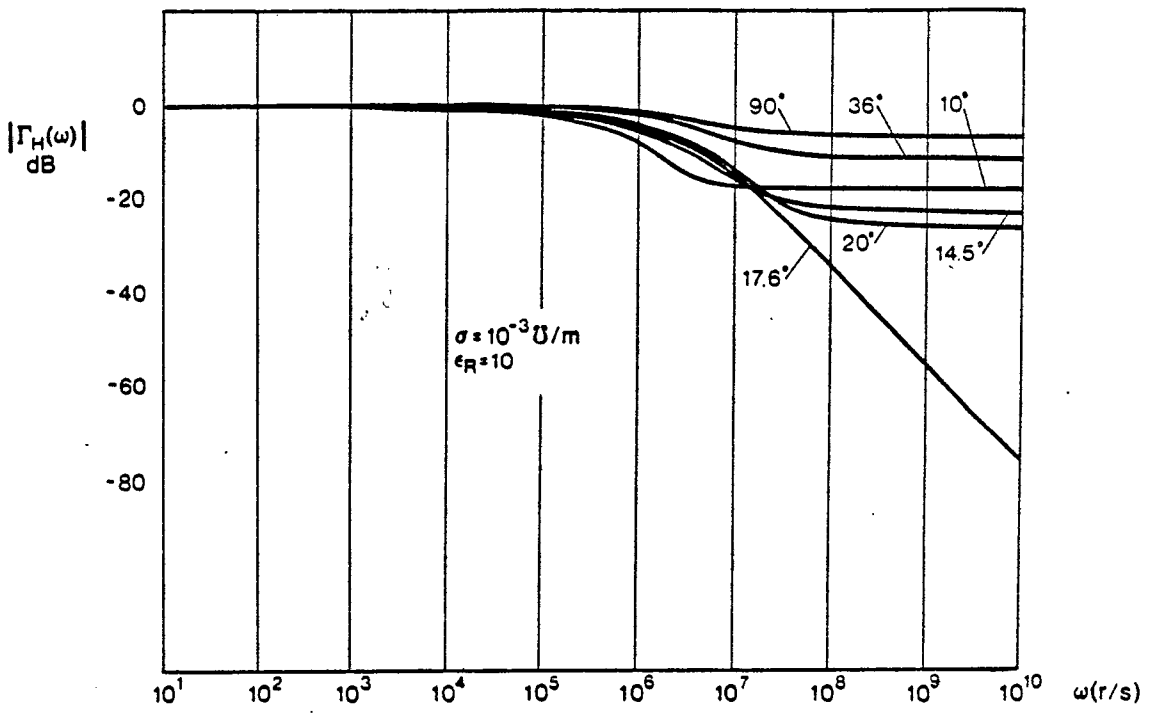

Figure A.10.

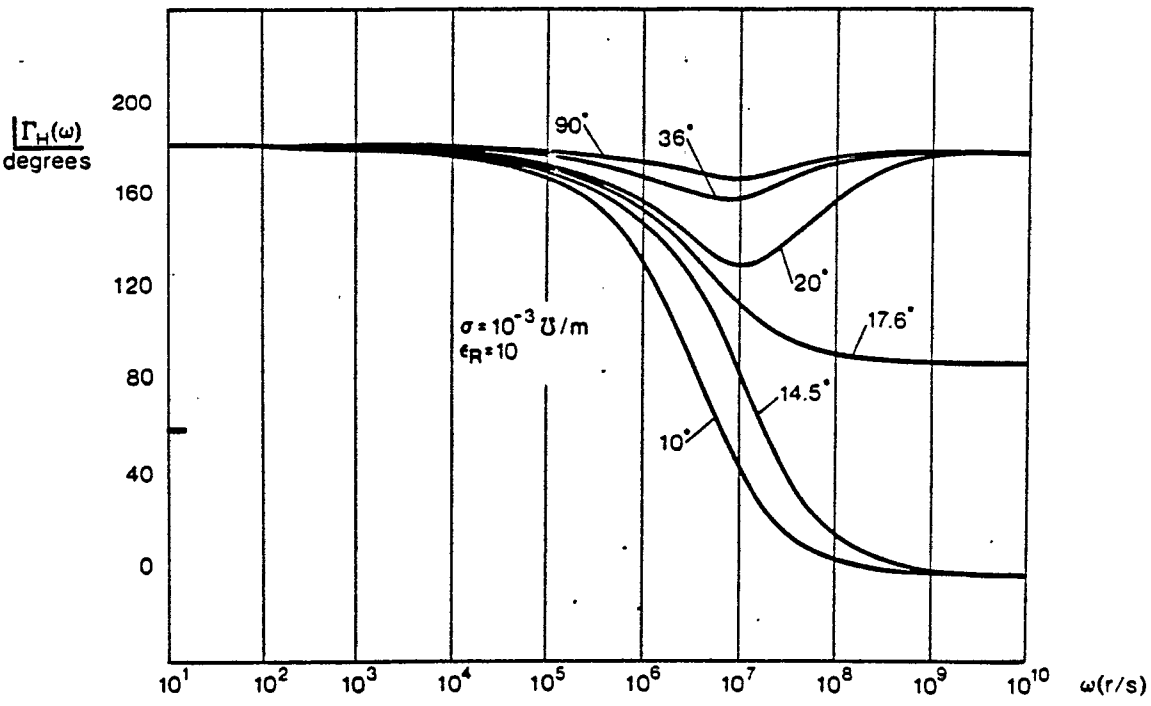

Figure A.11.

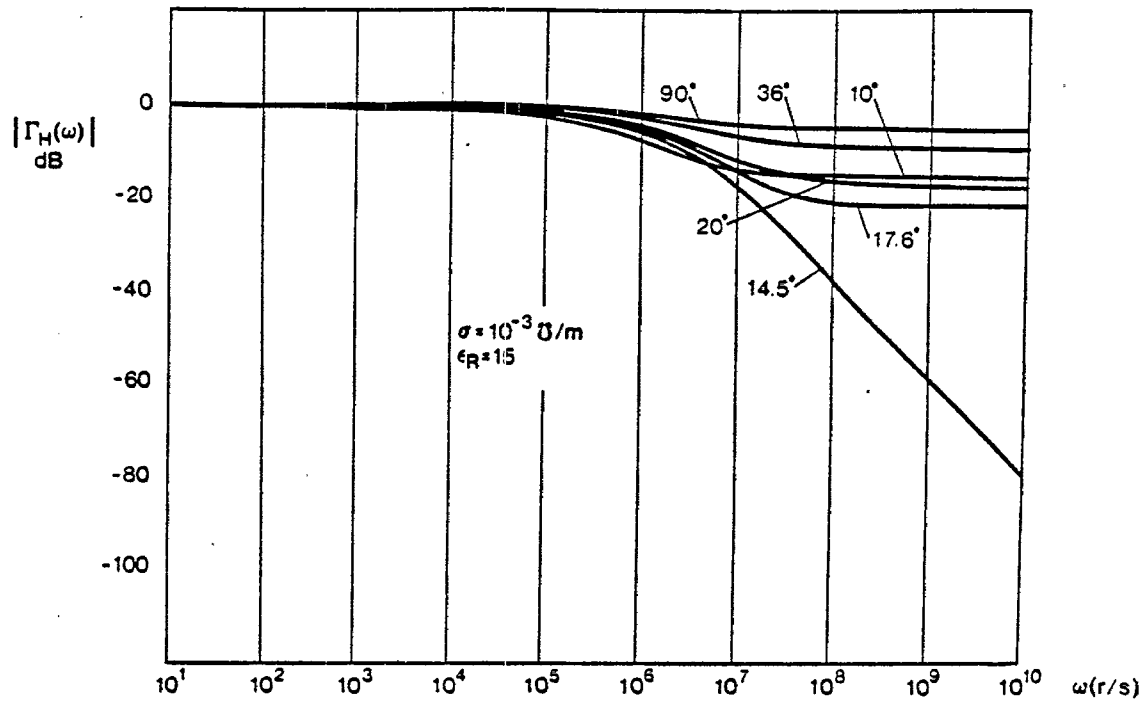

Figure A. 12.

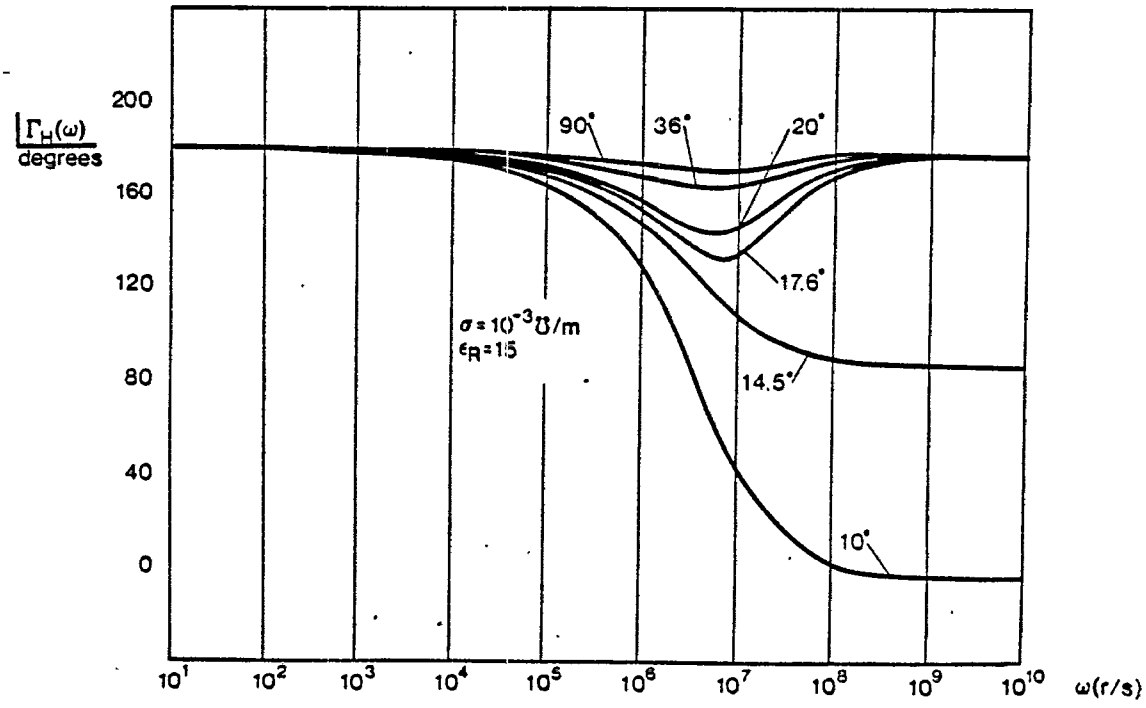

Figure A. 13.